

**OPTICAL SENSOR BASED SURFACE PLASMA RESONANCE  
(SPR) WITH IOT FOR SOLUTION CONCENTRATIONS  
DETECTION**

**MUHAMAD IRFAN BIN HASSAN NUSI**



**UNIVERSITI TEKNIKAL MALAYSIA MELAKA**

**OPTICAL SENSOR BASED SURFACE PLASMA  
RESONANCE (SPR) WITH IOT FOR SOLUTION  
CONCENTRATIONS DETECTION**

**MUHAMAD IRFAN BIN HASSAN NUSI**

**This report is submitted in partial fulfilment of the requirements  
for the degree of Bachelor of Electronic Engineering with Honours**

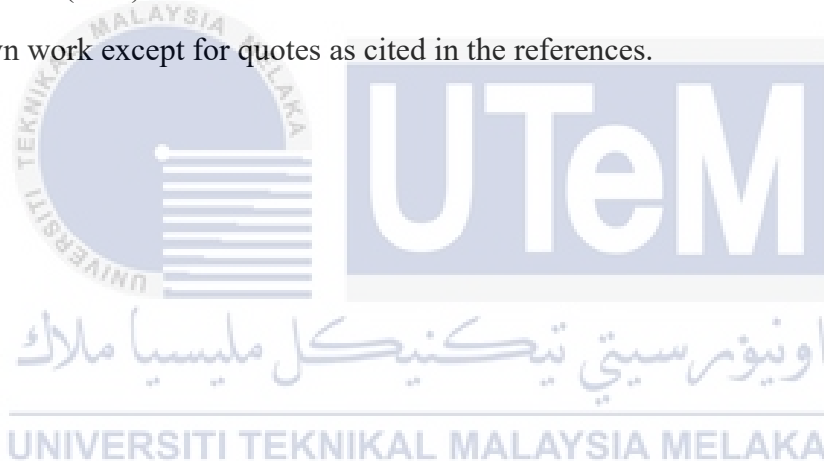


**Faculty of Electronic and Computer Engineering  
Universiti Teknikal Malaysia Melaka**  
UNIVERSITI TEKNIKAL MALAYSIA MELAKA

**2022**

## DECLARATION

I declare that this report entitled "Optical Sensor Based Surface Plasmon Resonance (SPR) With IoT for Solution Concentration Detection" is the result of my own work except for quotes as cited in the references.



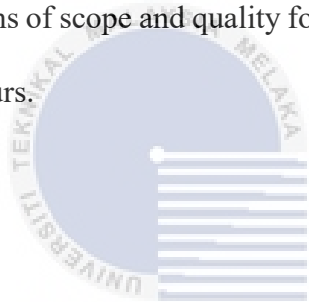
Signature : .....

Author : MUHAMAD IRFAN BIN HASSAN NUSI

Date : 12 JANUARY 2022.....

## APPROVAL

I hereby declare that I have read this thesis and in my opinion this thesis is sufficient in terms of scope and quality for the award of Bachelor of Electronic Engineering with Honours.



اونيورسيتي تيكنيكل مليسيا ملاك

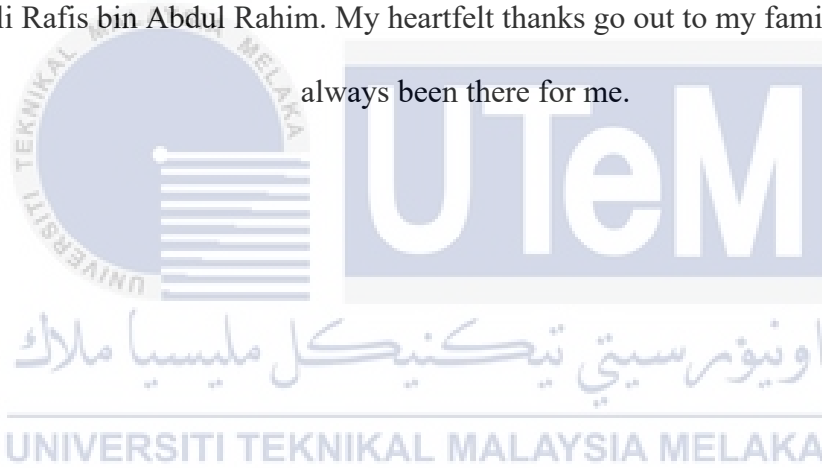
Signature : .....

Supervisor Name : .....

Date : 12 JAN. 2022 .....

## DEDICATION

This project was a great success thanks to God and my wonderful supervisor, Dr. Hazli Rafis bin Abdul Rahim. My heartfelt thanks go out to my family, who have always been there for me.



## ABSTRACT

The present work describes a compact and cost-effective optical sensor based on surface plasmon resonance (SPR) for sensing various concentrations of saline solution. This project utilises a red LED as the light source, gold-coated glass substrates as SPR chips, a Nodemcu to power the LED and an op-amp to amplify and display the output voltage, as well as six different concentrations of saline solution. This methodology is divided into two distinct phases: Final Year Project 1 and Final Year Project 2. The initial phase involved testing the designed light source and photodetector circuitry using the SPR chip. It was used to verify that the photodetector could detect the red LED and to record the output voltages. After that, the designed circuit was integrated with the IoT platform. The second phase involved the analysis of saline solutions.

## ABSTRAK

*Kerja ini menerangkan sensor optik padat dan kos efektif berdasarkan resonans plasmon permukaan (SPR) untuk mengesan pelbagai kepekatan larutan garam. Projek ini menggunakan LED merah sebagai sumber cahaya, substrat kaca bersalut emas sebagai cip SPR, Nodemcu untuk menghidupkan LED dan op-amp untuk menguatkan dan memaparkan voltan keluaran, serta enam kepekatan larutan garam yang berbeza. Metodologi ini dibahagikan kepada dua fasa yang berbeza: Projek Tahun Akhir 1 dan Projek Tahun Akhir 2. Fasa awal melibatkan ujian litar sumber cahaya dan pengesan foto yang direka bentuk menggunakan cip SPR. Ia digunakan untuk mengesahkan bahawa pengesan foto boleh mengesan LED merah dan untuk merekodkan voltan keluaran. Selepas itu, litar yang direka telah disepadukan dengan platform IoT. Fasa kedua melibatkan analisis larutan garam.*

## ACKNOWLEDGEMENTS

All gratitude to Allah for providing me with the opportunity, determination, and strength necessary to accomplish my Final Year Project (FYP) and this thesis. Throughout my life and research period, His unending kindness and mercy were with me. My supervisor, Dr. Hazli Rafis Bin Abdul Rahim, deserves special recognition for his excellent supervision and unwavering support. Throughout my research, his great knowledge in this sector has served as a source of encouragement and inspiration.

Additionally, I would want to express my gratitude to all photonics laboratory members at Universiti Teknikal Malaysia Melaka (UTeM) for their kind support, assistance, and making the lab a pleasure to work in despite the hectic and challenging nature of the research. I would like to express my gratitude to Muhammad Fahmi bin Hisamudin for his unwavering support throughout my research period.

Finally, I want to express my heartfelt appreciation to all of my family members for their patience and encouragement. Without their ongoing direction and assistance, this research would not have been possible.

## TABLE OF CONTENTS

<b>Declaration</b>	
<b>Approval</b>	
<b>Dedication</b>	
<b>Abstract</b>	<b>i</b>
<b>Abstrak</b>	<b>ii</b>
<b>Acknowledgements</b>	<b>iii</b>
<b>Table of Contents</b>	<b>iv</b>
<b>List of Figures</b>	<b>viii</b>
<b>List of Tables</b>	<b>xi</b>
<b>List of Symbols and Abbreviations</b>	<b>xii</b>
<b>List of Appendices</b>	<b>xiv</b>
<b>CHAPTER 1 INTRODUCTION</b>	<b>1</b>
1.1 Introduction	1
1.2 Problem Statement	2
1.3 Objectives of the project	3
1.4 Scope of the project	3

1.5	Hypothesis	4
1.6	Organization of the thesis	5
<b>CHAPTER 2 BACKGROUND STUDY</b>		<b>6</b>
2.1	Surface Plasmon Resonance	6
2.1.1	Introduction to SPR	6
2.1.2	Early History of SPR Biosensor	8
2.1.3	History of SPR Biosensor After 1990	9
2.1.4	Previous SPR Applications	11
2.1.4.1	Biomedical Applications	11
2.1.4.2	High-Throughput Screening (HTS)	11
2.1.4.3	Photonic Researches	12
2.1.4.4	Cellular Analysis and Cell-Based Detection	13
2.1.4.5	Biomedical applications of SPR with biosensors	15
2.1.5	Advantages Of SPR	17
2.1.6	The Principle Of Surface Plasma Resonance (SPR)	18
2.1.7	Surface Plasmon Resonance (SPR) Current Instrument	19
2.1.7.1	Examples of Fan-shaped Beam SPR Instruments	20
2.1.7.2	Examples of Fixed and Scanning angle SPR Instruments	23
2.1.7.3	Examples of Label-free Biosensing Instrument	25
2.1.7.4	Examples of SPR Imaging Instruments	27

	vi	
2.2	Optical Properties of Gold	29
2.2.1	Nanoparticles	29
2.2.2	Gold Nanoparticles	31
2.3	Light Emitting Diode (LED)	34
2.3.1	Working Principles of LED	34
2.3.2	Emission Of LED Lights	35
2.4	Photodetector Circuits of Sensor System	38
2.5	Sodium Chloride or Saline Properties and Uses	39
2.5.1	Sodium Chloride Properties	39
2.5.2	Sodium Chloride/Saline Solution Uses	41
2.6	Internet Of Things (IoT) Platform	42
<b>CHAPTER 3 METHODOLOGY</b>		<b>44</b>
3.1	Project Methodology	45
3.2	LED Light Source & Photodetector Circuit Design with Iot Platform	47
3.2.1	Optical Sensor Based SPR Circuit Fabrication	47
3.3	Fabrication for SPR chip	50
3.4	Optical sensor based SPR circuit IoT integration process	52
3.5	Solution Preparation and Sensing Process	55
<b>CHAPTER 4 RESULTS AND DISCUSSION</b>		<b>60</b>
4.1	Analysis of The Designed Circuit and Internet of Thing (Iot) Integration.	61

	vii
4.2 Analysis of The Optical Sensor Based SPR With IoT Platform for Solution Concentrations Detection	63
4.3 Sensing Mechanism	67
<b>CHAPTER 5 CONCLUSION AND FUTURE WORKS</b>	<b>69</b>
5.1 Future Works	70
<b>REFERENCES</b>	<b>71</b>
<b>APPENDIX I</b>	<b>76</b>
<b>APPENDIX 2</b>	<b>77</b>

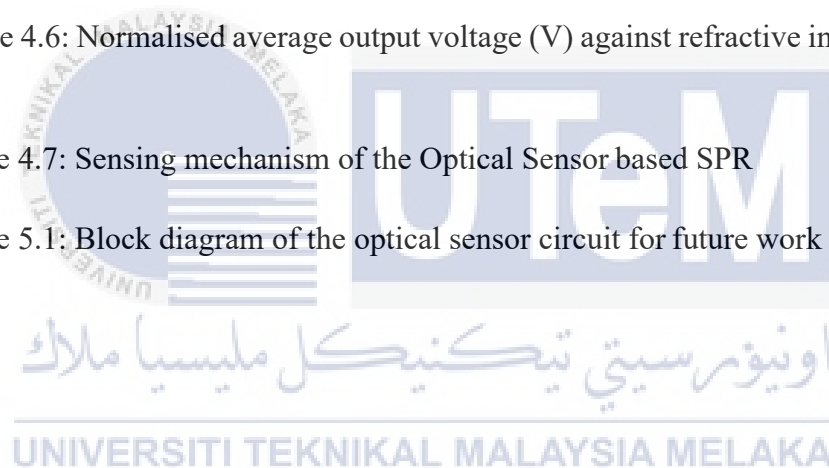


## LIST OF FIGURES

Figure 2.1: SPR papers recorded in PubMed [1]	7
Figure 2.2: SPR Imaging System	12
Figure 2.3: Sensor gram showing the evolution of resonance units (RU) versus time during association and dissociation measurements performed in the BIAcore instrument [5].	16
Figure 2.4: In the SPR product line of Biacore: X, 3000, S51, and X100, respectively.	21
Figure 2.5: Biosensing Instrument	22
Figure 2.6: Instrument of the SensiQ Technologies	23
Figure 2.7: Instrument for Analytical $\mu$ -Systems (BIOSUPLAR-6)	23
Figure 2.8: OpenSPR Instrument	24
Figure 2.9: The Indicator-G for Sensia research platform	25
Figure 2.10: LFIRE imaging system in the form of attenuated total reflection configuration	26
Figure 2.11: BiOptiX's 404pi enhanced SPR system	27
Figure 2.12: The SPRimager II of GWC Technologies. A spindle is used to manually set the SPR angle	27
Figure 2.13: EzPlex Instrument of Horiba Scientific	28
Figure 2.14: The PlexArray HT of Plexera LLC	29
Figure 2.15: Various shape of gold nanoparticles	31

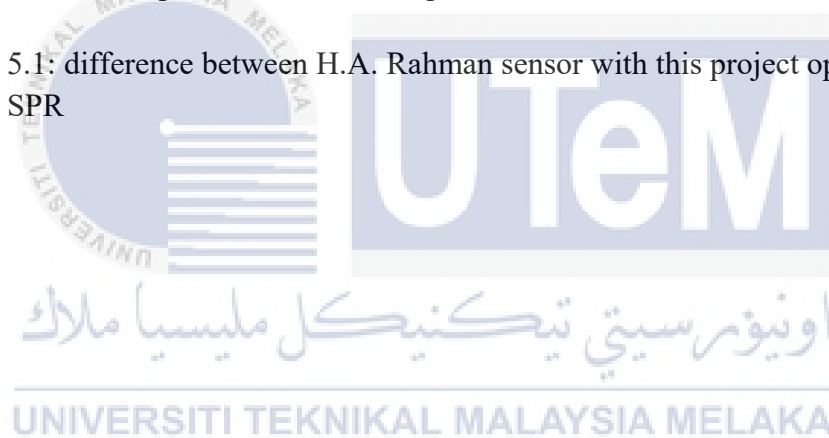
Figure 2.16: Electron's reaction in LED	35
Figure 2.17: Emission of LED	36
Figure 2.18: Photodetector circuit's schematic	39
Figure 2.19: Sodium Chloride Crystal Structure	40
Figure 2.20: Total Research regarding the IoT [11]	43
Figure 3.1: comparison of sensing sensitivity between 3 LEDs with and without polarizer	44
Figure 3.2: Sensitivity comparison between gold and silver	45
Figure 3.3: Project's Flowchart	46
Figure 3.4: Block diagram of the optical sensor based SPR with IoT	47
Figure 3.5: Standard schematic diagram of the optical sensor based SPR	48
Figure 3.6: Circuit layout that is printed on the UV Board	49
Figure 3.7: Printed circuit onto the UV board	49
Figure 3.8: Optical sensor based SPR circuit configuration	50
Figure 3.9: SPR chip's size and coating technique	51
Figure 3.10: Machine used for coating SPR chips	51
Figure 3.11: Some of the command lines developed in Arduino IDE software	52
Figure 3.12: Blynk App with the SuperChart function	53
Figure 3.13: Export function in the Blynk app	54
Figure 3.14: Flowchart (continued)	55
Figure 3.15: Sodium Chloride and De-ionized Water	56
Figure 3.16: The bottles for storing different salinity concentrations	56
Figure 3.17: Scale for measuring the Sodium Chloride	57
Figure 3.18: Heating Magnetic Stirrer	57

Figure 3.19: Digital Refractometer	58
Figure 3.20: Demonstration of the solution dropping onto the SPR chip	59
Figure 4.1: Circuit's Configuration	61
Figure 4.2: The interface of the Blynk app with the running data received from the optical sensor circuit	62
Figure 4.3: Array of received output voltage	63
Figure 4.4: Normalized average output voltage against salinity solution concentration (g)	64
Figure 4.5: Normalized average output voltage against salinity solution concentration (%)	65
Figure 4.6: Normalised average output voltage (V) against refractive index unit (RIU)	66
Figure 4.7: Sensing mechanism of the Optical Sensor based SPR	68
Figure 5.1: Block diagram of the optical sensor circuit for future work	70



## LIST OF TABLES

Table 2.1: Various type of medical application with the saline solution	41
Table 3.1: Salinity solution with different concentrations and its RIU	59
Table 4.1: The performance of the optical sensor on the salinity solution	66
Table 4.2: Sensor performance of the optical sensor with the refractive index	67
Table 5.1: difference between H.A. Rahman sensor with this project optical sensor based SPR	70



## LIST OF SYMBOLS AND ABBREVIATIONS

SPR	:	Surface Plasmon Resonance
LED	:	Light Emitting Diode
LCD	:	Liquid Crystal Display
IOT	:	Internet of Things
HTS	:	High-Throughput Screening
VEGF	:	Vascular endothelial growth factor
MALDI	:	Matrix-assisted laser desorption/ionization
TIR	:	Total Internal Reflection
DNA	:	Deoxyribonucleic Acid
PCB	:	Printed Circuit Board
RIU	:	Refractive Index Unit
UV	:	Ultraviolet

## LIST OF APPENDICES

Appendix A: Formula used in analysis.....	77
Appendix B : Coding for Nodemcu.....	78



# CHAPTER 1

## INTRODUCTION



### 1.1 Introduction

This research is mainly about the experiment regarding the detection of the optical sensor-based Surface Plasmon Resonance (SPR) in different concentration of the saline solution. Generally, optical sensors can detect and quantify a variety of light properties, including intensity, frequency, wavelength, and polarisation. Light detectors that can transform light into electrical impulses are used in these sensors. As for the Surface Plasmon Resonance, it has been one of the best methods that has drawn massive attention from various party because of its extensive applications in the field of chemical sensor as well as the biosensor. In simple terms, SPR is a phenomena that occurs on a metal surface when light strikes it at an angle that was employed for incident light in this experiment with reference to earlier studies at an angle of 30. However, there is still an obstacle to commercialization of SPR due to the mass and

cost of the present SPR instruments. It also has been the reason of this research which to create a cost-effective optical sensor-based SPR. Besides, the solution used in this experiment will be Sodium Chloride or saline solution. This solution is widely used for the production of the furniture, building materials, interior decoration and household products such as detergent, glues, some paints, medicines and vitamins. That is one of the reasons why this research is introduced which to detect the concentration of the salinity within a specific area in order to avoid any danger whenever someone is being exposed to the solution. This experiment will include some of the equipment that has been considered to be the best setup to optimize the final result of the experiment such as gold substrate for the coating of the glass debris and red colour of the Light Emitting Diode (LED) for the light sources on the optical sensor. LED is determined to be the best light sources for this experiment because it has an advantages in term of costing and availability.

## 1.2 Problem Statement

As being said before, the current Surface Plasmon Resonance (SPR) instrument used in the industry is bulky because it is combined with several other component such as the prism, the waveguides and the other optical component. In addition, the present instrument also needs a mechanical aid component that would be responsible for aligning the SPR system, including the rotational stage. This situation will affect the final building cost of the instrument to be more expensive which is one of the downsides of this sensing system. Additionally, the saline solution utilized in this experiment is known as normal saline. Physiological or isotonic saline is sometimes referred to as such. Our daily lives could not function without the countless uses of saline. Numerous medical applications include the removal of dead skin cells, the

cleaning of sinuses, and the treatment of dehydration.. But, excessive amount of salinity in one solution can give some side effect when apply to human such as fever, injection swelling and redness. That is the reason why the concentration of this saline solution needs to be monitored thoroughly and the optical sensor based SPR is one of the best mediums that can be used to do so.

### 1.3 Objectives of the project

Saline solution sensing is the primary goal of this research study, which will examine the feasibility of using an inexpensive and simple optical system based on SPR. Sub-goals include the following:

- i. To design an LED light source and photodetector circuit for an SPR concept based on an optical sensor.
- ii. To integrate the designed optical sensor based SPR concept with the IOT platform.
- iii. To conduct an experimental analysis of the optical sensor-based SPR with an IoT platform for the detection of saline solution concentrations.

### 1.4 Scope of the project

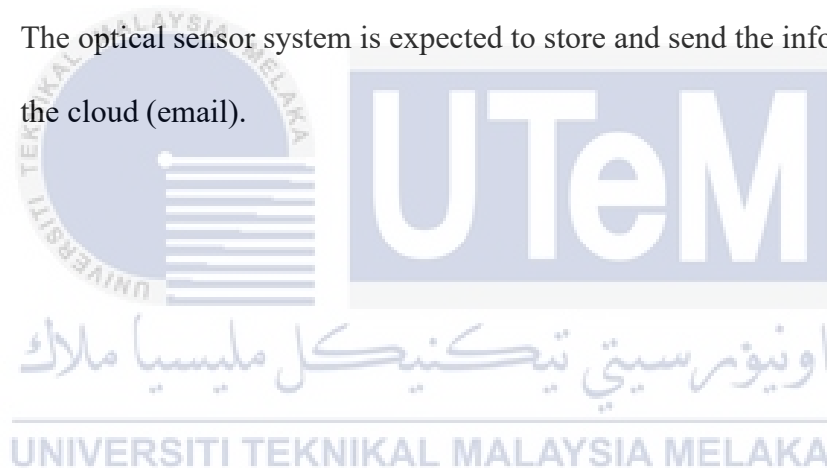
This project requires SPR chips, which are glass substrates covered with a 30nm layer of gold. For the light source, red LED will be used. The light beams from the LED will be reflected on the SPR chip and then received by the photodetector before it sends the information to the NodeMCU to produce an output in term of voltage value that later will be shown on the LCD and in the email platform as this project includes the IOT. The SPR chips will be a sensing platform to react with droplets of the saline

solution as it is the main target to be sensed in this research study. The solution is prepared with several different concentrations in order to gain its refractive indexes. There are also four other parameter that will be analyze which are sensitivity, standard deviation, linearity and resolution in order to determine the sensing performances.

### 1.5 Hypothesis

There are three major hypothesis that can be listed for this research study:

- i. When sensing various saline concentrations, the SPR chip is expected to exhibit a range of sensing capabilities.
- ii. The optical sensor system is expected to store and send the information into the cloud (email).



## 1.6 Organization of the thesis

Chapter 1 provides an overview of this work, outlining the project's aims and scope of the research study, as well as the problem statement, hypothesis, and project's objectives and hypothesis. Chapter 2 presents a theoretical assessment of related research, including an in-depth examination of optical sensor-based SPR technology, its idea, and applications. Additionally, this chapter describes the characteristics of gold substrates used in SPR. This article reviewed a study on the use of LEDs as light sources in an optical sensor-based SPR idea. The final section of this chapter discusses salinity sensing with optical and electrical sensors.

Chapter 3 details the methods used to accomplish the objectives of this project, which is separated into three sections. The first is to create LED light sources and photodetectors based on SPR idea for the optical sensors. Secondly, integrate the designed optical sensor based SPR concept with the IOT platform which in this case e-mail will be used as the medium. The final methodology is to conduct an experimental analysis of an optical sensor-based SPR paired to an IOT platform for the purpose of detecting solution concentrations.

Chapter 4 examines and analyses the sensing data for various saline solution concentrations using a gold SPR chip illuminated by a red LED. Graphs and tables illustrate the findings. Chapter 5 concludes with a conclusion and suggests additional research to improve the proposed technique.

## CHAPTER 2

### BACKGROUND STUDY

#### 2.1 Surface Plasmon Resonance

##### 2.1.1 Introduction to SPR

The number of papers including data obtained from commercial biological sensors climbed to more than 20 000 by 2016 in 1990, following the introduction of the first commercial surface Plasmon Resonance (SPR) device (Biacore) (PubMed data) [1], as shown in Figure 2.1 below:

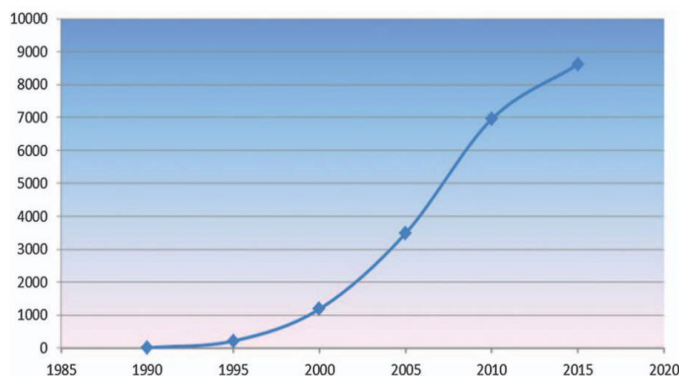


**Figure 2.1: SPR papers recorded in PubMed [1]**

The increase in detection sensitivity from 108 RIU (refractive index unit) by nearly 100 times has not only contributed to the number of publications, but has also contributed to improvements in resonance or response technology. In 1990 four channels (Biacore), the number of independent channels or spots in the newest IBIS MX96 imaging device increased to at least 192 flow-regulated spots and over 10,000 ligands in SPR imaging devices from different manufacturers (e.g., Plexera) [1].

The 1990 carboxymethylated dextrane surface was added to a range of different surfaces [1] which is still the first option for many applications. Different fabricators have produced specialized application systems as complements to all-intentional research instruments, and SPR biosensors are continuously increasing their effect on biomolecular interaction studies. With increased experimental design and updated data analysis methods, high-quality data may be collected for determining kinetic parameters of biomolecular interaction events. These findings offer additional insights into not only the affinity of eight biomolecular couples, but also molecular binding event mechanisms, which are vital to unravel the interesting processes in living things for functional protein interaction trials.

### 2.1.2 Early History of SPR Biosensor

After being discovered by Wood in 1902[1,] the physical phenomenon of SPR found its way into useful applications in sensitive detectors capable of identifying sub-monomolecular protein coverage. The physical representation of SPR has been found to be capable of detecting proteins' sub-monomolecular scope in multiple applications on sensitive detectors.

The use of SPR-based sensors in monitoring biomolecular interactions was demonstrated in 1983 by Liedberg, Nylander, and Lundstro'm and later by the Linko'ping Technology Institute (Sweden) in their quest for label-free, real-time biomolecular sensing [1]. They collected human immunoglobulin G (IgG) on a 60 nm silver film to detect a 60 nm silver film. Other physical techniques, such as ellipsometry, refractometry, and photothermic detection, were used to investigate the intrinsic properties of the molecules, such as mass, refractive index, and/or charge distribution. At the Swedish National Defense Laboratory, the relationships between proteins have been monitored in real time, without the use of labels, using ellipsometry. The refractive index change on a light-reflecting surface would have been most notably the transducer's operating mechanism. A drawback to the ellipsometer's ability to detect variations in refractive index resulting in the formation of biomolecular structures upon this optical transducer substrate surface would be that light can pass through the volume of the sample solution, making it difficult to accurately measure specimens something which absorb light or includes particles.

The University of Twente (Netherlands) has also worked on a search for new transduction principles for the detection of immunocompromised transistor responses (immunoFET) and Immunochemical Optical Biosensor (IMOB) surface among other

research laboratories [1]. Direct optical transmission of biomolecular binding events has been demonstrated through optical transducer ideas such as ellipsometry, SPR, and interferometric principles (Mach Zehnder). In the mid-1980s, successful immunochemical measurements of reactions with SPR were carried out and published.

In a six-year programme of development, Pharmacia Biosensor chose SPR as its platform for direct biomolecular contact sensing and resolved fluid and surface chemistry issues [1]. The liquid handling device has advantages in terms of design freedom because of the setup of Kretschmann. The higher refractive index medium blocks light from passing through the fluid (the prism), instead it is reflected on the sensor surface, shielded by a thin metal sheet. Gold was recognised as SPR's greatest inert metal film, whereas silver gives physically greater SPR effects [1].

For the production of microfluid flow channels, procedures for etching silica were devised to build a casting mould. The creation of optogels between the prism of the optical unit of the instrument and the sensor chip also took place. The optogel ensures optical communication with the prism, which allows the sensor chip to be quickly replaced. These research and development operations were aimed at converging three unrelated areas of research, optics, microfluidics and surface chemical sciences and culminated in the active creation of the instrumental concept of biomolecular interaction analysis (BIA).

### **2.1.3 History of SPR Biosensor After 1990**

Pharmacia Biosensor launched the first commercial SPR product, the Biacore instrument in 1990 [1]. The SPR was the most modern, sensitive, precise,

reproducible, direct, label-free biosensor technology, and the "gold standard" for the measurement of real-time biomolecular interactions. To compete with the Biacore technology, Fisons Instrumenty has used evanescent field technology, known as echoing mirror technology, which is not basically SPR, to investigate bio-molecular interactions.

In 1995, IBIS Technologies introduced a single-channel, cuvette-based SPR system. The device was compatible with the Biacore sensor chip, but optically with the scanning angle concept. IBIS II, a two-channel cuvette based SPR device powered by auto samplers, was released in 1997. IBIS Technologies has begun production of the SPR imaging instruments following the combination with sensor surface coating company Ssens BV, in 1999. The creation of a cuvette replacement with a specific back-and-forth cell system took several years for Biacore to establish high standards for the accurate detection of biomolecular interactions.

While the history of the 25 manufacturing enterprises' SPR and SPR-like instruments cannot be completely recounted, the Biacore Product line's history is very straightforward. This dissertation is not intended to give an exhaustive discussion of SPR's physical theory. Instead, it is intended to provide people involved in SPR work with a low threshold introduction of SPR physics and wish to understand more than "measure SPR-dip shifts."

## 2.1.4 Previous SPR Applications

### 2.1.4.1 Biomedical Applications

SPR biosensing tends to be one of the best ways to control the binding affinity of biomolecules and screening of primary medicinal molecules. SPR type sensors are rapidly being employed in the field of biomedical science in order to research several biological creatures, such as DNAs, RNAs, proteins, carbohydrates, lipids and cells.

### 2.1.4.2 High-Throughput Screening (HTS)

The application extensions of SPR Biosensors are not restricted to complex ligand-receptor interaction kinetics studies; they are also employed for drug discovery and drug production. There is numerous various SPR biosensor format, including the multi-canal unit format, the SPR image format, allowing simultaneous and continuous analysis of the output of hundreds and thousands of affinity binding events on a chip surface.

Biomolecules on gold surfaces are computed as reflective changes with regard to the strength of the incident ray in SPR images, unlike SPR sensors that use an angle of SPR measurement or an SPR wavelength absorption dip to measure biomolecules on a gold surface. It is possible to perform multiplex analyses using a surface plasmon resonance (SPR) biosensor, but this is not possible with normal SPR instruments because there are only four studies that can be performed simultaneously.

SPR imaging technology, on the other hand, provides a multi-analyte biosensor high-performance approach and provides a sensitivity that is similar to typical SPR biosensors. Therefore, SPR imaging systems without labelling criteria are more

suitable for high performance screening (HTS). In 2004, Maillart et al. established an SPR imaging system-based HTS technique for numerous interaction studies between the p53 transcription factor and its associated cis-acting DNA components. In 2007, Neuman et al. established a technology that could detect interactions of up to 9216 target lines on a single array [8].

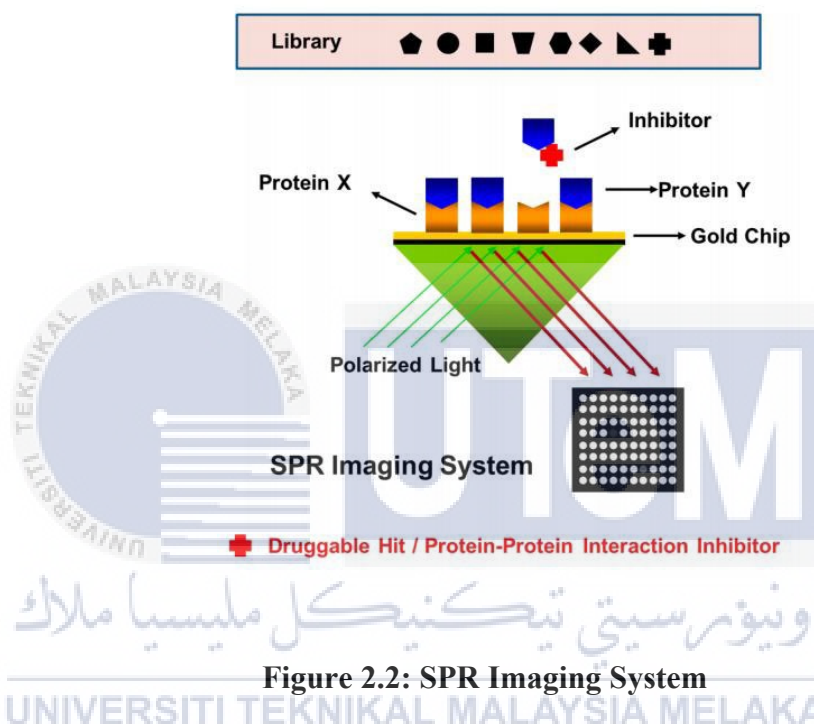


Figure 2.2: SPR Imaging System

Drug screening at a high throughput employing an SPR imaging protein chip device. On a gold surface, the brilliant picture represents protein-protein interaction. Protein-protein interactions are disrupted when an inhibitor binds to the target protein, resulting in changes in the SPR imaging signal intensity and a darker picture [8].

#### 2.1.4.3 Photonic Researches

Methods for biomarker identification and analysis have acquired increased interest and rapid progress in the areas of proteomics in recent years. For outbreaks of such diseases to be predicted, biomarkers must be recognised and diagnosed so that surgery and other unneeded and costly medical interventions for individuals might be

prevented. Therefore, additional research is required to identify novel biomarkers and develop new technologies for faster and more reliable detection. Due to their low concentrations and the small size of their separate matrices, identifying and quantifying 13 biomarkers is typically difficult. Accurate screening procedures suitable for clinical use are often difficult to identify and verify. SPR has proven effective when diagnosing biomarkers because of its sensitivity, mobility, obviation of high sample numbers and multiplexed detection capabilities. Many diseases, including breast, ovarian, and pancreatic cancer, along with cardiac and neurological ailments, have been effectively diagnosed using SPR biosensors.

#### **2.1.4.4 Analysis of Cellular Structure and Cellular Detection of Pathogens**

The SPR approach is helpful not only because of its in-time and non-label imaging capability to dynamic surface changes, but also for cellular changes, such as physiology, cell-surface interactions and cell detection [8]. The SPR approach enables cellular response, cellular adhesion and cell products, as well as cancer cells and bacterial cells to be monitored. After receiving a reactive molecular stimulation, mammalian cells respond appropriately. As a result, the SPR signal fluctuates in response to cell-molecule interactions. A 2007 study by Yanase et al., which found a large resonance angle shift (AR) in the SPR sensor when rat-2H3 mast cells and PAM212 cells (mouse keratinocyte cell lines) were grown and triggered on a sensor chip using an epidermic growth factor (EGF) or antigen [8]. These findings show that AR alterations constitute intracellular events other than changes in the region of the cell adhesion. The SPR signal was also used for cell growth and size changes calculations [8]. Exposure to non-isotonic stimuli can cause cell volume to alter. In

particular, hypotonic stimulation leads to a drop in the SPR signal, and the signal reverses to an equilibrium value if more isotonic solutions are introduced.

The SPR technology plays a crucial role in cancer cell detection. The initial strategy was the development of cancer biomarkers using monoclonal antibodies that have been immobilised on the sensor surface. The second method explicitly tests cellular response for quantitative analysis. Cancer cells are directly on the sensor surface planted and grown. Next, liquids that include stimuli circulate through cells and their reaction is calculated in real time by means of SPR. This procedure has been effectively utilised to identify and detect malignant tumour cells such as Chinese hamster ovary cells without the use of immunological markers. Liu et al. built a surface mounted SPR bio sensing device with anti-VEGF antibodies and alive SKOV-3 cells cultivated on the cells' cell flow ceiling. Cancer cells began generating VEGF in the action that supported the growth of blood vessels. Such generated VEGF then generated unique attachments with the antibody down on the chip surface and recorded the SPR signal.

The new technology allows VEGF sensitivity to be detected in real time with a linear dynamic range of  $0.1\text{-}2.5 \mu\text{g}\cdot\text{mL}^{-1}$  [2]. In 2006, a group identified an integrated method by utilising surface plasmon resonance imaging (SPRI) and a microwave gold protein chip. They were able to use this approach to do recombinant E. coli cultivation and identification and purification on the protein chip. The process involved inducing proteins on a microwave chip, E. coli cell lysis (by inserting lysozymes), purifying glutathione S-transferase-fused vertebral fluorescent protein (GST-GFP) by means of affinity interaction with the gold surface chip and, finally, identifying the proteins used by the SPRI procedure. The microwave chip was

constructed with a PDMS elastomer connected to a gold surface providing a 36-wave chip with a sample volume of 5  $\mu$ L for each well.

#### **2.1.4.5 The use of SPR biosensors in biomedical applications**

Affinity parameters for biological interactions are frequently discovered using biosensing SPR sensors. Immobilized ligands or binding proteins upon that sensor chip are paired with their binding partners in the buffer that flows past it. The buffer maintains a steady concentration of the binding partner, making it easier for the two to bind. Flow changes to a buffer with no interacting molecules when equilibrium is reached. It disrupts the harmony and separation between both the two parties that are bound together. Analyte-binding residue is removed by cleaning the sensor chip and then repeating the procedure inside the buffer with various concentrations of the binding partner. Figure 2.3 shows how the tool records sensor program RU changes that occur during connection and detachment as depicted by the tool.

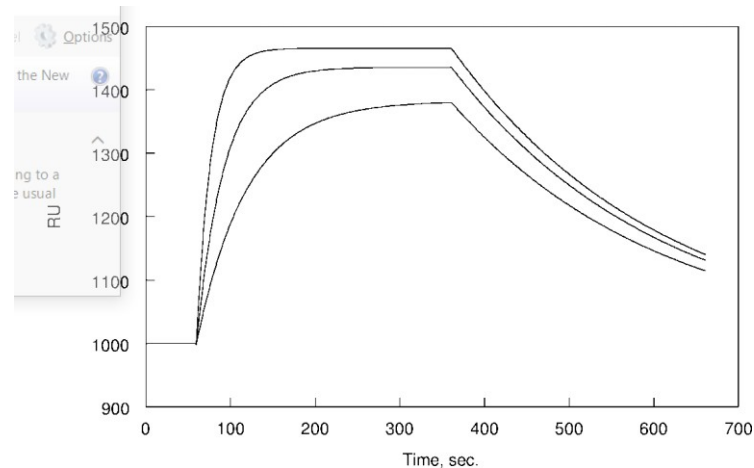


**Figure 2.3: Associative and dissociative BIAcore equipment illustrates the progression of resonance units (RU) over time [5].**

Adequate processing of data can be used to determine the constants of association and dissociation and therefore the constant affinity of the relation. The methodology offers many advantages over standard techniques of measuring affinity. It requires little material, is very fast and requires no tracer labelling. An important drawback is the necessity to recycle the sensor chip for readings at various concentrations. Several techniques were proposed for this problem, including the use of multi-channel instruments and the use of the analyte concentration gradient in single-channel devices in the buffer flow. The application of classical SPR to affinity measurements has found a niche in numerous fields of biomedical science. However, SPR measurements are sensitive not only to changes in the medium's refractive index around the sensor, but also to changes in the sensor layer thickness. As any changes in the protein conformation might lead to changes in this parameter, SPR has also been widely employed for the analysis of the conformation of immobilised proteins in different settings.

In conjunction with flight mass spectrometry matrix-assisted laser desorption/ionization times, the latest developments in the classic SPR are in the area

of proteomics (MALDI-TOF) [5]. By integrating these two approaches, SPR improves the investigation of biomolecular interactions between molecules, at least one of which is recognised. It is usually not known whether a protein mixture is used during the interaction analysis. MALDI-TOF thereby distinguishes the molecule from the mixture, which interacts with the sensor.

The combination is particularly successful, as the metal layer takes part in the laser desorption/ionization process. However, MALDI-direct TOF's implementation on the sensor chip is damaging. In recent advances, novel sample anchoring supports for the MALDI-TOF approach have therefore been used to allow elution and further identification of the binding partner from the SPR instrument. This allows a regeneration of the sensor chip. The continued rise of SPR applications in biomedical sciences during the previous decade illuminates the many promises made by the method. More recently, a new perspective has been opened for SPR with their application in the bio-physical characterisation of binding and structural events occurring in biomembranes, enabling a deeper and more complicated knowledge of the particular and unspecific cell interactions.

### **2.1.5 SPR's Advantages**

Many biosensing devices are available, SPR technology facilitates and accurate observation of binding behaviour on a molecular level than ever before. Here are only a few clear benefits related to the utilisation of surface plasmon resonance. SPR has a detection without a label. Variations in the refractive index are established using

SPR such that no label is required for detection. You may see biomolecular interactions in real time between a number of proteins, DNA/RNA and small molecules.

Next, SPR requires a minimum number of samples to undertake experiments. Scientists and health practitioners can use cheaper materials, save money and make surface plasmon resonance more accessible and usable. Apart from that. Another economic advantage of SPR is the ability to reuse sensor chips. Sensor chips affect the quality of the data directly and act as a critical biosensing component. It is even more astonishing because those chips can be reused, relying so much on the quality and performance of the sensor chip. SPR can also repeat measurements.

Finally, the use of SPR technology is essentially an easy and somewhat inexpensive technique to see how different biomolecules interact in real time. The applications here are tremendous in the realms of genetics, kinetics and the pharmaceutical and medical sectors. Also increasing areas of interest are new material applications, such as nanoparticles.

#### **2.1.6 The Principle Of Surface Plasma Resonance (SPR)**

Polarized light arrives at the interface of two transparent media, such as the glass prism and buffer solution, from the media side with the highest refractive index. When light is monochromatic, it is reflected and refracted partially onto the interface plane.

However, all light is reflected beyond a specific angle of incidence and none of them is refracted. Total Internal Reflection (TIR) [2] is this phenomenon. The Au (gold) film in SPR is covered with a glass prism. Free electrons in the conduction of

metals generate periodic oscillations, known as plasma waves. This can also, like every periodic electromagnetic wave, be represented in a particle way. A plasmon is the name of the plasma wave particle, as are the particle names for light and sound waves, photons and phonons.

Ground plasmons are plasmons that are restricted to the surface of the metal. It occurs on the Au (gold) surface and buffer interface. These plasmons create an electrical field that extends roughly 100 nm into the buffer solution as well as the Au (gold) film and glass prism. This electric field is called an evanescent wave, because it declines exponentially with time [4]. When the light stream has the proper angle of incidence inside the TIR, surface plasmon resonance occurs (total internal reflection). At the 'resonance 19 angles,' the photons in the beam are equivalent to the momentum (vector of magnitude and direction) of the surface plasmons, and the photons are converted to plasmons. In other words, optical energy is coupled with the Au (gold) surface. The reflection is diminished at this angle of resonance.



### **2.1.7 Surface Plasmon Resonance (SPR) Current Instrument**

Numerous SPR tools are currently accessible from a variety of sources. Even while it is hoped that the coverage of commercially available instruments would be substantial, the value of technology on the market for diverse purposes cannot be assessed by reference to the relative amounts of text given to them here. There may also be other approaches for detecting biomolecular interactions in real time that are not reliant on the SPR phenomena or use a different configuration. This is exemplified by FOX Diagnostics' development of a commercial fiber-optic SPR system.

## 2.1.7.1 Examples of Fan-shaped Beam SPR Instruments

### 2.1.7.1.1 GE Healthcare

Over 80 percent of installed products and 87 percent of publications in 2015 were from the Swedish company Biacore, which was bought by GE Healthcare in 2006 and now controls the SPR business and sets industry standards. Biacore's engineers have relied on the fan-shaped SPR instrument concept since the company's inception in 1990. When using a Biacore device, a light emitting diode ( $\approx 760$  nm) is employed, and an exact spot on the sensor's surface is used to reflect a converging beam of light. A line can be detected on the sensor surface by extending the light fan into a wedge and employing a two-dimensional detector. Using a light fan with a linear array detector eliminates the need for any moving parts when performing an SPR test. A computer programme using unique fitting routines calculates the mathematical minimum down to the size of a single diode. A 0.001-millimeter dip in the SPR dip is possible with the SPR dip accuracy. Sensor chip and cylindrical prism are optically matched using an optogel. Various probes mounted at certain points along a line are used to assess multiple biomolecular interactions simultaneously. Numerous microfluidic cartridge-connected flow cells are used by Biacore. Figure 2.4 shows some of the older Biacore machines.



**Figure 2.4: In the SPR product line of Biacore: X, 3000, S51, and X100, respectively.**

#### 2.1.7.1.2 Biosensing Instrument with SPR

The BI-SPR (BI4500 series) from Biosensing Instruments (Tempe, AZ, USA) detects the SPR angle using a diverging beam approach (Figure 2.5). The SPR-dip position on the detector's surface changes when the SPR angle changes. All flow channels can be utilized in conjunction with two valves to simultaneously measure two samples. Alternatively, one channel might be used for context subtraction. The device comprises a range of cell modules that may be utilized for protein-protein interactions, DNA sequencing, ligand-receptor recognition, and drug development. The extra cell module isn't included in the base device when doing electrochemical SPR experiments.



**Figure 2.5: Biosensing Instrument**

### 2.1.7.1.3 SensiQ Technologies with SPR concept

As of 2007, SensiQ Technologies (Oklahoma City, OK, USA) has been developing the pioneering range of SPR instruments. Many Pioneer models and all FEE models employ the unique OneSteps injection method, which incorporates the SensiQ technology (Figure 2.6). Using Taylor dispersion, it is possible to create a gradient of analyte concentration for a single injection to offer a high-resolution dosage response. The screening of low molecular weight fragments is enhanced greatly by a method utilised expressly for this purpose. Analyte diffusion coefficient and heterogeneity or aggregation of analyte can be determined using this technique. It was first referred to as the TDi injection technique in 2012, but has subsequently been renamed OneSteps. SPR with stepped gradient injections according to a predetermined profile is another dynamic injection SPR (diSPR) concept, and it is patented in the local dilution method FastSteps. Along the way to the flow cell, the analyte concentration is adjusted. Low molecular weight applications benefit from a sample productivity boost of more than tenfold when compared to conventional techniques.



**Figure 2.6: Instrument of the SensiQ Technologies**

### 2.1.7.2 Examples of Fixed and Scanning angle SPR Instruments

#### 2.1.7.2.1 Analytical m-Systems

When Analytical m Systems/Mivitec GmbH launched the BIOSUPLAR series in the late 1990s in Sinzing, Germany, it was a huge success. Development of the third generation (BIOSUPLAR-6) is presently underway (Figure 2.7). Differential measurements are possible using the unit's two optical channels, which can also be utilised as a reference channel. Training for new SPR users and lessons can be done with a simple setup. The SPR market's most cost-effective instrument is the lightweight device, which can compete with Nicoya's OpenSPR.

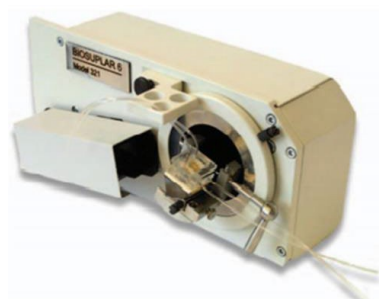


**Figure 2.7: Instrument for Analytical  $\mu$ -Systems (BIOSUPLAR-6)**

### 2.1.7.2.2 Nicoya

The OpenSPR instrument from Nicoya (Kitchener, ON, Canada) (Figure 2.8) uses the localised SPR (LSPR) idea to analyse gold nanoparticles immobilised on the sensor surface without the use of a label. Sophisticated spectrophotometers are able to detect changes in resonance wavelength. The 10 RU scale measures sensitivity. An extremely basic sample injection setup is provided by the instrument. It is the most affordable SPR instrument on the market, costing between \$10,000 and \$15,000. A new version of OpenSPR, OpenSPR XT, has been unveiled by Nicoya as an automated version of the platform.



**Figure 2.8: OpenSPR Instrument**

### 2.1.7.2.3 Sensia

Figure 2.9 shows the Kretschmann [1] setup used by the Sensia Indicator-G research platform in Madrid, Spain, to achieve conditions of total internal reflection resonance. User-friendly, but difficult to operate from a technological standpoint due to beam splitter alignment and light steering through a small flow cell. The

corporation, on the other hand, has overcome these technical difficulties.

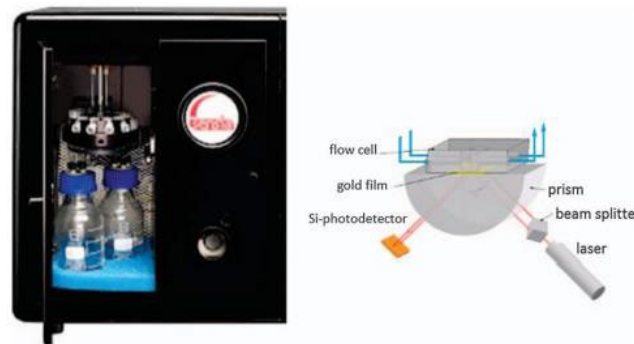


**Figure 2.9: The Indicator-G for Sensia research platform**

### 2.1.7.3 Examples of Label-free Biosensing Instrument

#### 2.1.7.3.1 Neosensor

Cambridge, UK-based Affinity Sensors created the IAsyS system, which was eventually purchased by NeoSensors, in the mid-1990s as a cuvette-based alternative to Biacore devices. [1] (Sedgefield, UK). It is true that this resonant mirror technique does in fact not use SPR, but it may be a label-free real-time alternative. It is mentioned in passing because of the impact it had on the 1990s. For reasons including sensor drift and difficulties with the instrument's cuvette construction, NeoSensors decided to halt the production of this instrument in 2011.

#### 2.1.7.3.2 Maven Biotechnologies

An example of a non-SPR instrument is illustrated in Figure 2.10 by Maven Biotechnologies (Pasadena, CA, USA) [1.] This instrument can be used to measure real-time interactions between biomolecules in a microarray or well-plate format. Biomolecules can include proteins, lipids, nucleic acids, small compounds like

medicines or steroids, or even whole cells. Ellipsometry, a technique based on measuring changes in light polarisation caused by reflection at the interface between two materials, provides the basis for the LFIRE test method. The optical set-up is identical to that found in Kretschmann SPR equipment of the same ilk (Figure 2.10). Biomolecular interactions can be studied "in real time" with this approach, which monitors reactions as they occur.

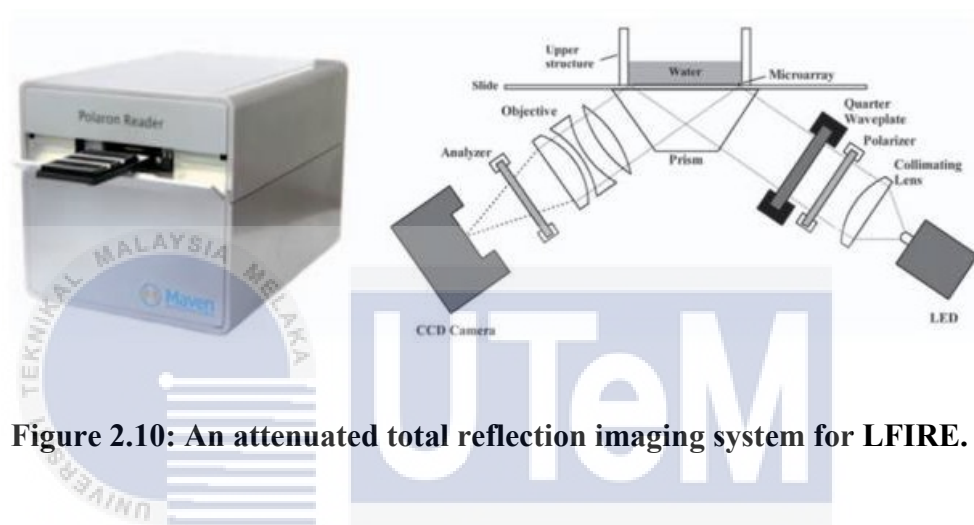


**Figure 2.10: An attenuated total reflection imaging system for LFIRE.**

### 2.1.7.3.3 BiOptiX

Low-noise and high-sensitivity instruments are available at a fraction of the cost of comparable systems because to BiOptiX' enhanced SPR technology (Figure 2.11). It also has high dependability, user-friendly experimental software, and a wide range of experimental capabilities. Incorporating interferometry and the SPR phenomenon, the BiOptiX 404pi provides an innovative and dependable detection method known as "Enhanced SPR". BiOptiX is a low-cost option for biomolecular interaction label-free real-time detection in drug discovery applications.



**Figure 2.11: BiOptiX's 404pi enhanced SPR system**

#### 2.1.7.4 Examples of SPR Imaging Instruments

##### 2.1.7.4.1 GWC Technologies

Figure 2.12 of GWC Technologies (Madison, WI, USA) shows the SPRImager II CCD camera, which simultaneously records data on the sensor surface. The SPR-left dip's flank angle is manually set at a fixed angle. Only one spot (such as a reference spot) can have the optimal angle chosen for maximum reflectivity, not all of them at once.



**Figure 2.12: The SPRImager II of GWC Technologies. A spindle is used to manually set the SPR angle**

#### 2.1.7.4.2 Horiba Scientific

SPRi-Lab+ and SPRi-Plex models of GenOptics have been licenced to Horiba Scientific (Longjumeau, France) for international distribution. Later, Horiba Scientific bought GenOptics (Orsay, France) for its laboratory instrumentation for high-performance testing systems beyond SPR. The Kretschmann arrangement is integrated to the Horiba high-end device EzPlex (Figure 2.13) and XelPlex systems, as well as the instrument is equipped with a spinning mirror to fix the incident angle on the flank of the SPR reflectivity dip.



**Figure 2.13: EzPlex Instrument of Horiba Scientific**

To monitor protein-protein interactions, this scan selects the sensor chip's optimum average reflectivity output in real time. A fixed angle is chosen for a specific point, and indeed the reflectivity of the point is tracked in real time. A broad beam of monochromatic polarised light illuminates the entire functionalized zone of the SPRi-Biochip, that includes a detection chamber. Information can be gleaned immediately from the contact phase while 29 tracks reflectance fluctuations against time.

### 2.1.7.4.3 Plexera LLC

PlexArrays HT, a high-throughput biomolecular interaction detection platform based on surface plasmon resonance imaging (SPRi) technology, was developed by a Lumera spin-off business, Plexera LLC (Woodinville, WA, US). The PlexArrays HT is a fully integrated platform that may be used to examine tens, hundreds, or even thousands of biomolecular interactions simultaneously (Figure 2.14). Over traditional protein array methods, KX Array Technology offers significant advantages over those that require additional labelling and produce just qualitative end-point data.

This technology reduces the data bias that is caused by label-based detection methods for absolute and relative affinities, specificities, and concentrations for quantitative analysis.



**Figure 2.14: The PlexArray HT of Plexera LLC**

## 2.2 Gold's Optical Properties

### 2.2.1 Nanoparticles

Optical and electrical qualities that are not present in bulk materials can now be achieved in nanoscale materials because to advances in nanoscience and nanotechnology. Various electrical and optical devices have made use of these

nanomaterial features that are size dependent. Researchers have also been working hard to figure out how nanoparticles work as a group and how to keep track of that data. According to a recent study, metallic nanoparticles' optical characteristics are largely dependent upon their surface plasmon, which refers to free electron oscillations within the metallic nanoparticle [4]. Nanoparticles, metallic species, and the surrounding environment all have an effect on the plasmon's resonant peaks and line widths [4]. It is only in the nanoscale range where these phenomena are discovered that the intrinsic and extrinsic size effects on the plasmon bandwidth can be explained. The extrinsic impact can be explained by quantum confinement of free electrons, size-dependent shifts in band structures, as well as inhomogeneous polarization and excitation of multipole modes [4]. In the presence of two nanoparticles, the plasmons' coupling is distance-dependent. The system's optical properties are determined by the optical properties of the individual particles and the electrodynamic interactions between them. The optical spectrum is determined by interparticle spacing, particle size and shape, and the dielectric medium. The plasmonic properties of individual nanoparticles and their pairs have already been studied extensively in both experimental and theoretical settings, but the existence of nanoparticle pair plasmons is still a mystery. It was predicted that the red and blue shifts in the extinction peaks of metallic nanoparticle dimers would diverge from those of single nanoparticles due to the plasmon energy of metallic nanoparticle dimers, as studied by Nordlander and coworkers [4]. In Chumanov's group [4], silver nanoparticle film electrodynamic particle coupling has been proven and used in the development of biosensory applications.

### 2.2.2 Gold Nanoparticles

The qualities of gold nanoparticles are distinct from those of bulk gold, which is solid yellow and inert in nature, whereas gold nanoparticles are anti-oxidant and are described as a wine-red solution. Interparticle interactions and the formation of gold nanoparticle networks play a critical role in determining the characteristics of these nanoparticles [7]. It is possible to obtain the gold nanoparticles in a range of forms and sizes (ranging from 1 nm to 8 m), including sphere, sub-octahedral, octahedron, decahedron and multiple twined polyhedrons as well as nanotriangles and hexagonal platelets (Figure 2.15).

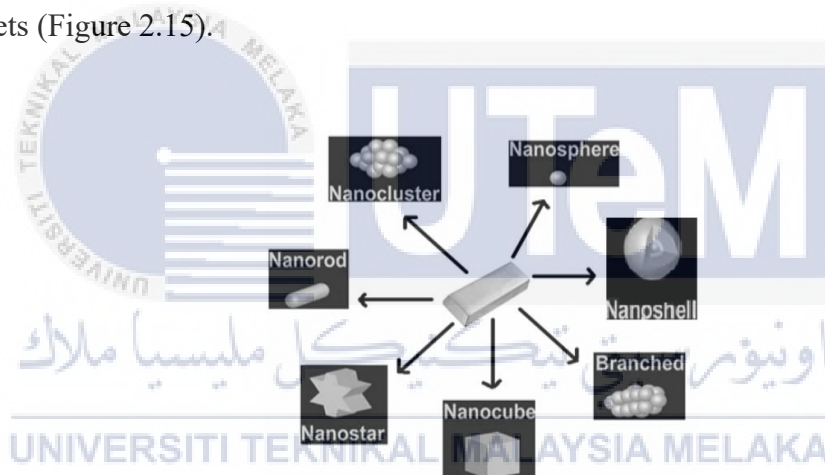


**Figure 2.15: Gold nanoparticles in a variety of shapes**

Triangular nanoparticles have the most appealing optical properties when compared to spherical nanoparticles. Gold nanoparticles are often used as a radiation enhancer in the field of radiation medicine [4] and also give a clinical benefit in radiation therapy by delivering drugs rapidly and selectively to the cancer location.. Gold nanoparticles have a variety of applications, including biomolecular ultrasensitive detection, killing cancer cells by hyperthermal treatment, identifying cells and proteins, and delivering therapeutic compounds into cells.

It is possible to use fluorescence or gold-based nanoparticles for molecular imaging of enzymes and metabolites that are essential for cancer cell function. Biological applications for gold nanorods have risen in recent years as a result of their unique optical and chemical features [4]. As a result of their unusual anisotropic structure, gold nanorods can absorb light at a range of wavelengths, including visible and near infrared (NIR). This makes them excellent for biosensors, gene delivery systems, and phototherapy. Because gold nanoparticles have a greater atomic number and electron density than iodine, they have a higher absorption coefficient than iodine, which improves CT contrast more than iodine, and have thus been utilized as molecular probes in X-ray CT imaging [4].

Non-cytotoxicity is a second major advantage of gold nanoparticles; their surfaces, which have a wide area, are excellent for biomedical modification with specific molecules or unique biomarkers. Since gold nanoparticles can be shaped, sized, and surface areas can be tuned, they play an important role in biology because of their compatibility and ability to be conjugated with proteins, as well as their unique optical properties. As a result of their vast surface area, shape, and crystallinity as well as their capacity to efficiently migrate into target cells and deliver significant drug loads [4], nanoparticles have been shown to be great therapeutic agents.

When it comes to medical research, gold nanoparticles are frequently used for imaging, medication administration and phototherapy as well as immunochromatographic identification of infections in clinical specimens due to surface plasmon resonance (SPR) [4]. These nanoparticles have unique physiochemical properties that make them ideal for gene transport; these include surface area, amphiphilicity and shape, biocompatibility, and surface carrier

capacities, as characterised by parameters such as protein structure, particle morphology, and conjugation approach [4]. The near infrared light dispersion and plasmon resonance absorption of gold nanorods allow for a wide range of in vivo imaging applications [4]. There has been a lot of interest in colloidal gold nanoparticles recently because of their small size, which is analogous to biological molecules like DNA and proteins, and the ease with which they can be prepared chemically [4]. A diameter of 18 nm gold nanoparticles has shown good penetration into cells, with no indication of injury, whereas a diameter of 1 nm gold nanoparticles can cross the cell membrane and nucleus to interact with DNA.

While gold nanoparticles have a high affinity for alkynes in comparison to other transition metal catalysts, homogeneous structures are neither commercially or environmentally viable due to the quick loss of active gold complexes to inert metallic gold during C-H alkyne activation. Due to the unique optical and electrical features of gold nanoparticles, color-indicating probes have been extensively exploited in the development of analytical techniques for multiple analyte sensing [4]. Gold colloids have been utilised to modify the surface of perfect electrodes due to their exceptional stability and unique features, including great biocompatibility, which is necessary to preserve the original structure and enzymatic function of attached proteins or enzymes. Combining gold nanoparticles with poly-like smart polymers (N-isopropylacrylamine) is an effective way to enhance the polymer's various features, such as its reversibility of collapse swelling in response to temperature stimuli [4].

## 2.3 Light Emitting Diode (LED)

The light-emitting diode, or LED, is a semiconductor diode that generates incoherent narrow-spectrum light when electrically biased in the forward direction of the p-n junction, as in the standard LED circuit. This is a form that is electroluminescent [10]. A LED is a light source with a small surface area, frequently with optics added to the chip to shape the emission pattern and aid in reflection. LEDs are also employed as a small indicator of lights in mobile devices and in higher-power applications such as flashlights and area lighting. Light Emitting Diodes (LEDs) are the most widely utilized form of semiconductor diode accessible today. When light emitting diodes are biased forward, they emit either visible light or invisible infrared light. Additionally, LEDs can be utilized as a standard domestic light source [3].

### 2.3.1 Working Principles of LED

The operation of a Light Emitting Diode is illustrated in Figure 2.3.1 (LED). The LED operates exclusively in the forward bias condition. When the LED is forward biased, the free electrons from the n-side and the holes from the p-side are driven towards the junction. When free electrons reach a junction or depletion zone, a portion of them reintegrate with the holes in positive ions. Because positive ions have fewer electrons than protons, they are more willing to receive electrons. Thus, at the depletion area, unbound electrons recombine with holes. Similarly, in the depletion area, holes from the p-side recombine with electrons. Due to the recombination of free electrons and holes in the depletion region, the diameter of the depletion area diminishes. As a result, more load carriers would pass via the p-n intersection.

Following that, recombination occurs in both the depletion field and the semiconductor p- and n-type. The unbound electrons in the conduction band release

energy in the form of light until they recombine with gaps in the valence band. The majority of energy is lost as heat in silicon and germanium diodes, and the output light is insufficient. However, the photons emitted have sufficient energy to generate extreme visible light in gallium arsenide and gallium phosphide [3].

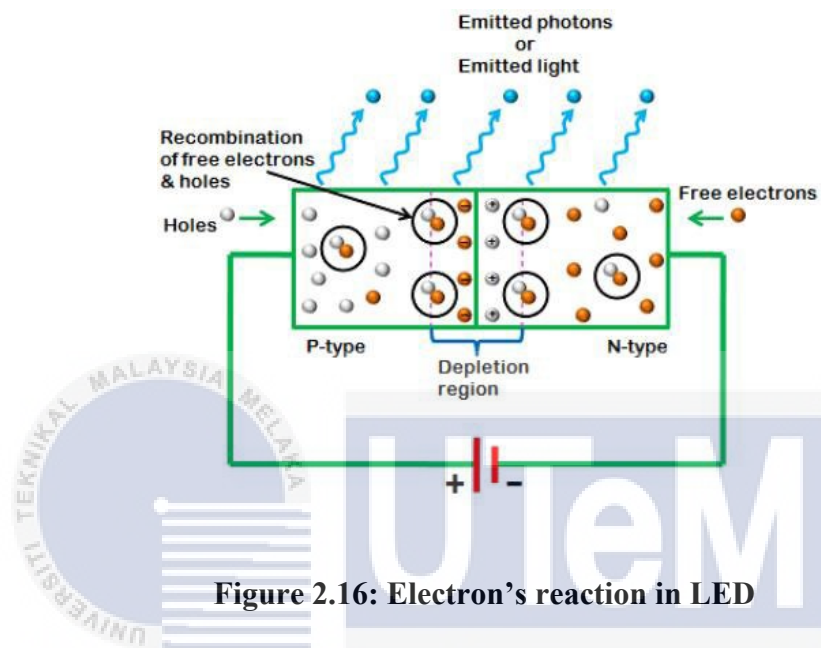


**Figure 2.16: Electron's reaction in LED**

### 2.3.2 Emission Of LED Lights

Fig. 2.3.2 illustrates the LED's emission mechanism. A voltage applied to the valence electrons causes them to separate from the parent atom, which is how LEDs get their energy. Because of their ability to break away from their parent atom, free electrons are sometimes referred to as valence electrons. They leave a hole in the valence shell created when the valence electron leaves the parent atom. A void is the term used to describe the space inside Valence's shell. All valence electrons have a virtually same energy level. Valence electrons' energy levels are assumed to be grouped together in the valence band spectrum. Similarly, the energy level of all unbound electrons is nearly identical. The conduction band is a term that refers to the

grouping of the energy levels of all free electrons in their spectrum. The energy level of free electrons in the conduction band is relatively high in comparison to the energy level of valence electrons or gaps in the valence band. Free electrons in the conduction band must consequently lose energy in order to recombine with the holes in the valence band. The free electrons do not persist in the conduction band for extended periods of time. After a brief length of time, the liberated electrons lose energy in the form of light and recombine with the holes in the valence band. Each time the charge carrier recombines, light energy is emitted.

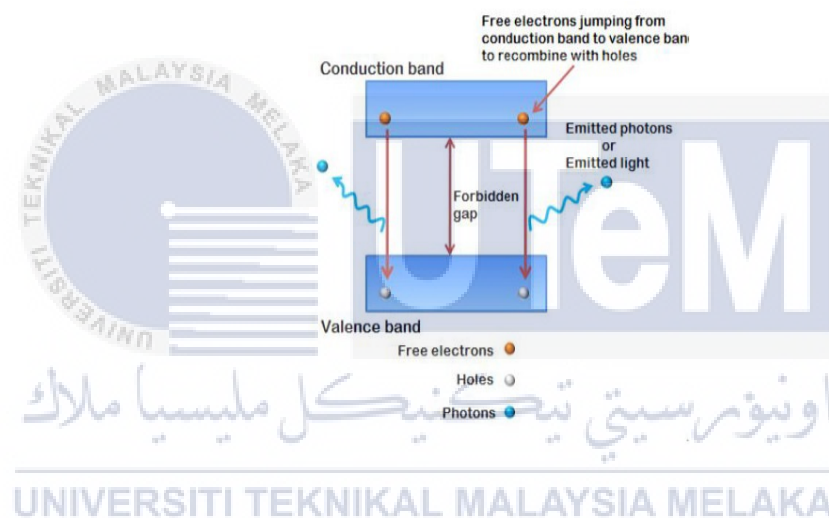


**Figure 2.17: Emission of LED**

The energy lost by free electrons or the intensity of the emitted light is proportional to the forbidden distance or energy gap between the valence and conduction bands. The semiconductor device with a wide prohibited gap emits high intensity light, while the semiconductor device with a tiny prohibited gap emits low intensity light. In other words, the intensity of the light emitted is determined by the material used to manufacture the LED and the forward current flowing through it.

In conventional silicon diodes, the energy difference between the conduction and valence bands is less. As a result, the electrons fall only a short distance away. As

a result, low energy photons are emitted. These low-energy photons have a low frequency and are therefore invisible to the human eye. Due to the large energy difference between the conduction and valence bands in LEDs, the free electrons in LEDs have a higher energy than the free electrons in silicon diodes. As a result, the unbound electrons fall across a large distance. As a result, high-energy photons are released. These high-energy photons have a high frequency that is visible to the naked eye. LEDs generate light more efficiently as the injected current increases and the temperature falls.

The recombination process produces light in light emitting diodes. Only in the presence of a forward bias does charge carrier recombination occur. As a result, LEDs operate solely in the forward bias direction. When the light emitting diode is reverse biased, the free electrons (majority carriers) on the n-side and the holes (majority carriers) on the p-side escape the junction. As a result, the width of the area of depletion grows and there is no charge carrier recombination. As a result, there is no generation of light. The system can also be influenced by a significant rise in the reverse bias voltage applied to the LED. Both diodes and photons emit light, although not all diodes emit visible light. The material used in an LED is selected so that the photons released have a wavelength in the visible region of the electromagnetic spectrum.

#### **2.4 Photodetector Circuits of Sensor System**

The lowest forward voltage ( $V_{fmax}$ ) and maximum forward current ( $I_{fmax}$ ) of the LED employed as a light source are 3.2 V and 20 mA, respectively. Reducing the LED current to a tolerable level requires a 100-ohm resistor linked in line with the

LED, which is powered by a 5 VDC supply from the Nodemcu board. This is to avoid the LED from catching fire. Ifmax was determined to be 18 mA using Equation (2.4).

$$I_{max} = \frac{V_{LED} - V_{f,LED}}{R_{LED}} \quad (2.4.1)$$

During sensor operation, light passes through the sample and the ZnO nanorods covered region. At the output, light is captured and converted to a linearly proportional current by the photodiode. Due to the photodiode's usage of a narrow aperture to filter stray light, the photodiode's light capture intensity is extremely low. As a result, a simple transimpedance amplifier (TIA) was utilised to transform the photodiode's output current to a processing voltage appropriate for the Arduino-based sensing system [13]. The receiver circuit is schematically depicted in Figure 2.4. It utilises an LT1884 op-amp chip (Linear Technology, 2000), which is a dual rail-to-rail output device with pico-amp input precision.

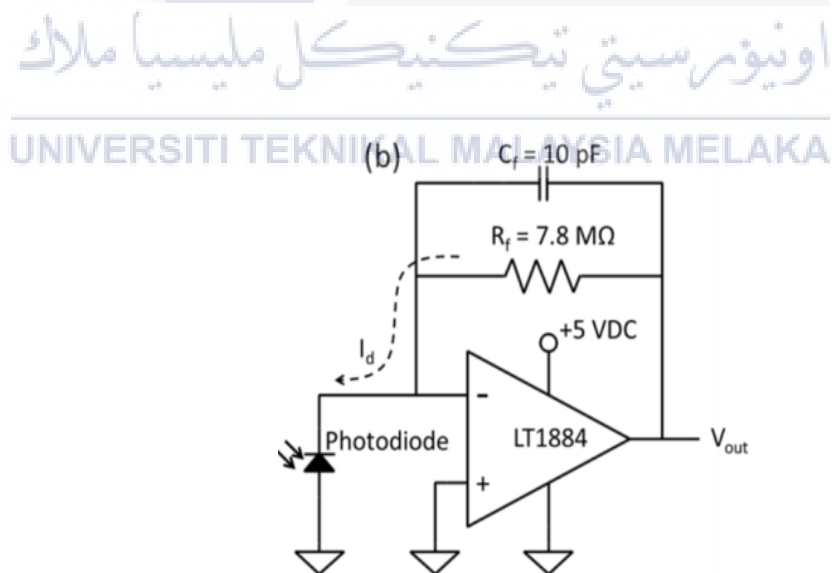


**Figure 2.18: Photodetector circuit's schematic**

The output voltage amplified by the operational amplifier can be expressed as

$$V_{000000} = R_f I_{id} \quad (2.4.2)$$

where  $R_f$  and  $I_{id}$  are the feedback resistor and photocurrent, respectively.

## 2.5 Sodium Chloride or Saline Properties and Uses

### 2.5.1 Sodium Chloride Properties

Sodium chloride dissolves readily in water and is insoluble or barely soluble in the majority of other liquids. It crystalizes into tiny cubic crystals that are transparent and colorless to white. Although sodium chloride has no odor, it does have a distinct flavor. It is an ionic compound composed of an equal proportion of positively and negatively charged sodium and chloride ions. By passing an electric current across it, sodium chloride can be broken down into sodium and chlorine [23], which is what happens when sodium chloride is melted or dissolved in water and the ions can readily move around. In addition, sodium chloride or saline solution is a solution composed of equal parts salt and water. The sodium chloride (salt) concentration in normal saline solution is 0.9 percent, which is comparable to the sodium concentration in blood and tears. Saline solution is frequently referred to as normal saline, however it is also known as physiological or isotonic saline [21].

Sodium chloride is actually a compound which 2 elements react together which are Sodium and Chlorine. It can be justified from the equation below:



As shown in figure 2.1.9, it is the sodium chloride crystal structure. Each atom has six nearest neighbours, with octahedral geometry. This arrangement is known as cubic close packed (ccp) [24].

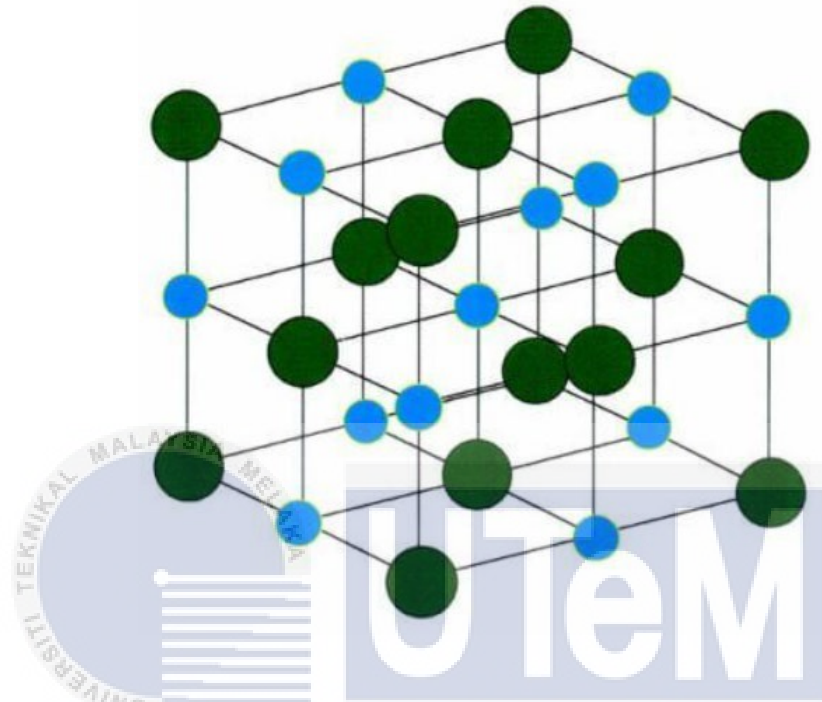


Figure 2.19: Sodium Chloride Crystal Structure

اوپنورسیتی تیکنیکل ملیسیا ملاک  
UNIVERSITI TEKNIKAL MALAYSIA MELAKA

### 2.5.2 Sodium Chloride/Saline Solution Uses

The most common form of sodium chloride is table salt, which is widely used in the food sector for flavouring and preservation. Additionally, it is used to manufacture a variety of vital compounds, including sodium hydroxide, sodium carbonate, baking soda, and hydrochloric acid. Additionally, it is used in oil refineries, textile mills, paper and pulp mills, fire retardants, the rubber sector, and road building. Another significant application is for de-icing roads and sidewalks in cold and snowy climates. Saline solutions are also employed in a variety of medical procedures [22].

There are numerous medical applications. It is applied to wounds, sinuses, and dehydrates people. It is offered as a topical cream or as an intravenous solution. While saline solution is easily available in pharmacies, it can be produced at home as well [21].

Medical uses for a saline solution include:

**Table 2.1: Various type of medical application with the saline solution**

Name	Use
IV drips	to treat dehydration and electrolyte imbalances; sugar can be added
Saline flush injections	to cleanse a catheter or intravenous line following medication administration
Nasal irrigation or nasal drops	to alleviate congestion, minimize post-nasal drip, and maintain the nasal cavity's moisture level
Cleaning wounds	to clean and rinse the area in order to maintain a sanitary atmosphere
Eye drops	help alleviate redness, tearing, and dryness of the eyes
Sodium chloride inhalation	to assist in the production of mucus in order to cough it up

## 2.6 Internet Of Things (IoT) Platform

The Internet of Things (IoT) refers to the networked interconnectivity of common things, many of which are endowed with omnipresent intelligence. By integrating every object for interaction via embedded systems, IoT will improve the Internet's ubiquity, resulting in a massively scattered network. A network of devices that communicate with each other and with humans. Rapid advancements in underlying technology have made it possible to achieve this [9].

Besides, The Internet of Things is an emerging topic of technical, social, and economic relevance. Consumer products, durable goods, automobiles and trucks, industrial and utility components, sensors, and other ordinary objects are being integrated with Internet connectivity and strong data analysis capabilities that promise to alter the way we work, live, and play. Projections regarding the impact of IoT on the Internet and economy are astounding, with some estimating as many as 100 billion linked IoT devices and a global economic impact of more than \$11 trillion by 2025 [10].

In recent years, the research area of the Internet of Things has witnessed transdisciplinary expansion and development. Various articles have been written quite extensively, covering different concepts and knowledge domains from technology, applied engineering, economics, business, strategy, industry, management, etc. This turns into a misunderstanding in comprehending the path of IoT knowledge development. Furthermore, IoT offers numerous dimensions disrupting people and nature, such as physical disorders in terms of work, cyberspace disruptions that deprive people of employment and face different new complexity in performing everyday activities and labor. At the same time, disruption to data by mastery of information generated by big data that gives rise to many new knowledge opportunities and changes new creative smart environment greatly in current circumstances (Ammirato et al., 2018), including interfering with many daily business processes in terms of people, skills and routine tasks aimed at benefits [11].

Most of the research is written on the use of IoT technology, runs as a way to facilitate human life in some areas, including how IoT contributes to corporate capabilities and newer investigations assess how data acquired from IoT devices might

benefit from different aspects. But to consider the extent of disruption that is extended throughout all industrial domains (so-called revolution) and is widely debated in the future under the fourth industrial revolution. It is a gap to construct a scientific thinking flow that handles this IoT growth and development that scientists, developers and companies may utilize. The direction to create IoT should be better understood, the nature and habits of the problem and the methodologies and instruments employed by researchers in the field of knowledge and industry.

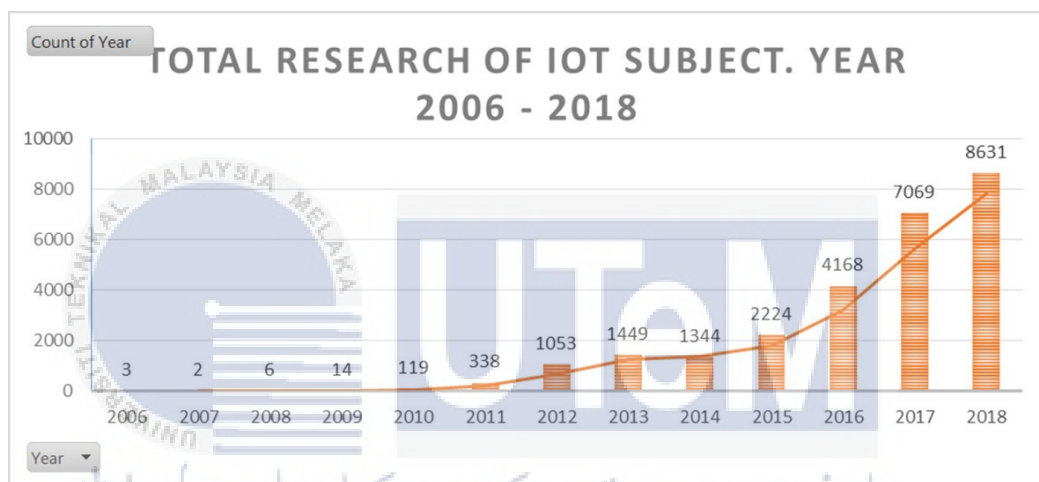


**Figure 2.20: Total Research regarding the IoT [11]**

## CHAPTER 3

### METHODOLOGY

This project is a continuation from the previous project done by the previous bachelor, Abdullah Yusof Bin Muhammad Anuar. His project includes several other results that conclude the optimal condition that can be used in the making of this optical sensor based SPR. For instance, his project has compared different color of the LED to observe which has the best sensitivity as shown in Figure 3.1 below.

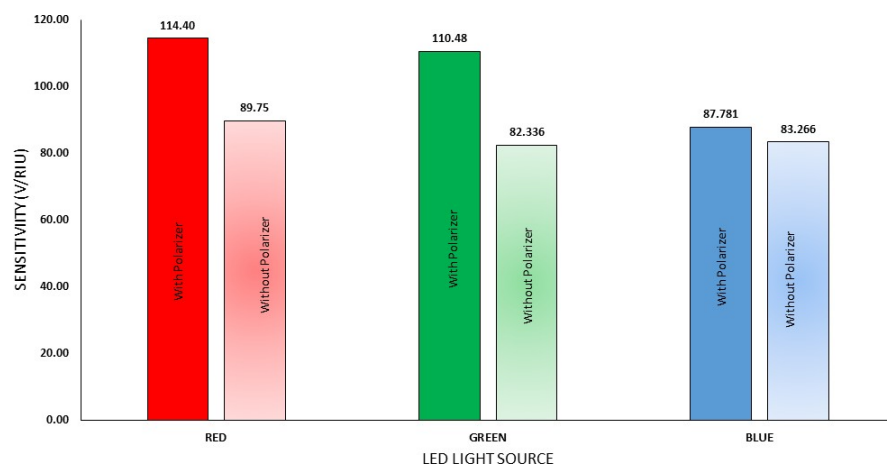


**Figure 3.1: comparison of sensing sensitivity between 3 LEDs with and without polarizer**

Based on the figure above, it has been justified that red LED has the best sensitivity among the other. Besides, in the figure also include the comparison between the LED that is equip with polarizer and without polarizer. The result from the figure indicates that polarizer significantly improved the sensitivity of the sensing performance. Therefore, red LED has been chosen as the light source and polarizer was used in the circuit configuration. Other than that, his analysis also includes the comparison of the SPR chips which one was coated with gold and the other was coated with silver. The analysis results shows that gold have better sensitivity than silver which can be observed from Figure 3.2 below.

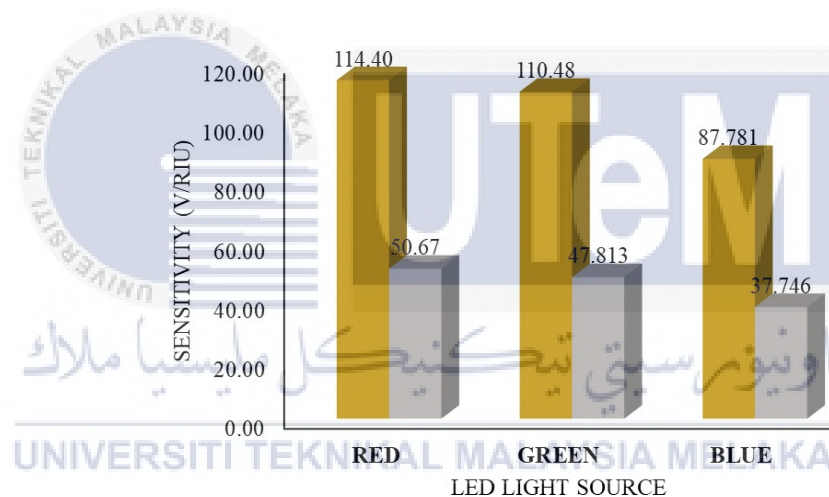


**Figure 3.2: Sensitivity comparison between gold and silver**

### 3.1 Project Methodology

The approach used in this research endeavor is explained in this chapter. Figure 3.3 depicts the approach flowchart for achieving the three research project objectives, which is separated into four primary procedures. Initially, an optical sensor-based SPR concept was designed with an LED light source and photodetector circuit.

Second, the IOT platform was integrated with the proposed optical sensor-based SPR idea. A 3D built framework to contain the SPR chip and LED light source was constructed using a 3D printer before the salinity sensing experiment.

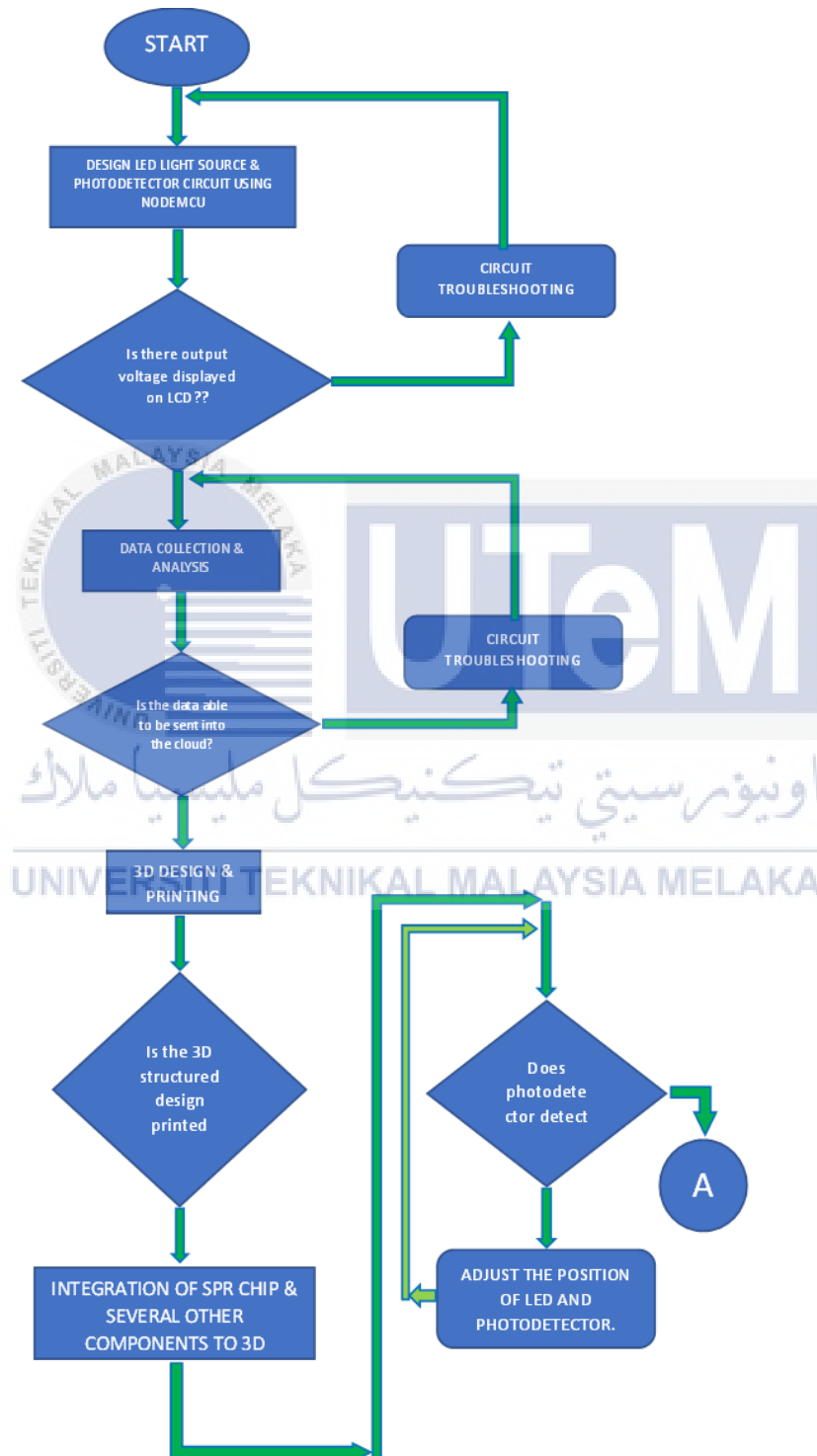


**Figure 3.3: Project's Flowchart**

### 3.1 LED Light Source & Photodetector Circuit Design with Iot Platform

The project started with the development of the circuit itself that requires several process including the designing, fabricating and sensing validation process. In the designing process, the circuit was created by using a block diagram as shown in Figure 3.4 below before it was designed in the Proteus software in order to fabricate the circuit onto the UV Board later.

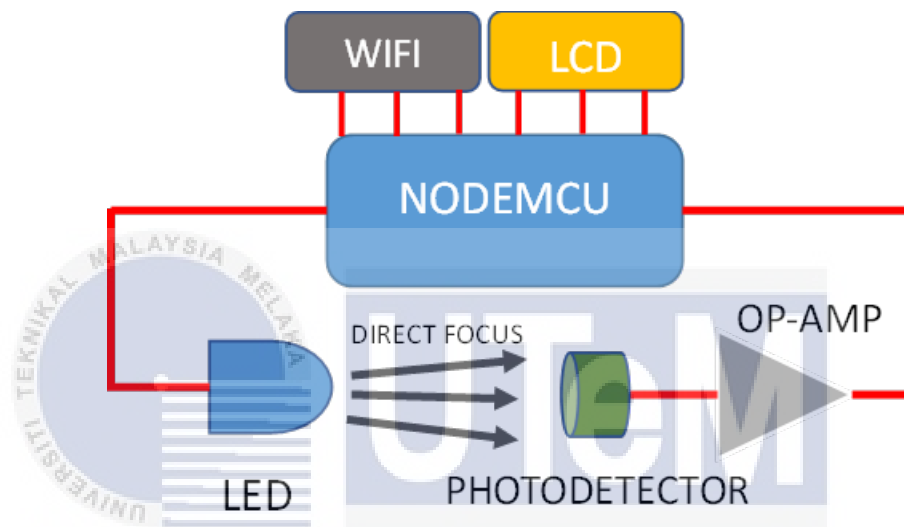


**Figure 3.4: Block diagram of the optical sensor based SPR with IoT**

#### 3.1.1 Optical Sensor Based SPR Circuit Fabrication

After the circuit has been finalized in the form of block diagram, the circuit is continued to be redrawn in the Proteus software accordingly to all specifications require for every component so that the circuit could work and give the expected output later. There were 2 types of drawing that needs to be done in the Proteus software. First was the standard configuration of the circuit while the other one was the layout of the circuit that will be printed on the UV board. Component connections between these two circuits are intertwined in a manner so critical that a single mistake

might cause the entire circuit to malfunction, or worse, stop working altogether. So, every connection was configured carefully to each end before developing the PCB layout afterwards. As depicted in Figure 3.5, connector J1 represent the pushbutton while connector J2 represent LCD display. Connectors were used in their place because the original components were not intended to be installed on the PCB board in the future. This means that another component with the same schematic footprint was substituted, in this case the connector, which worked perfectly.

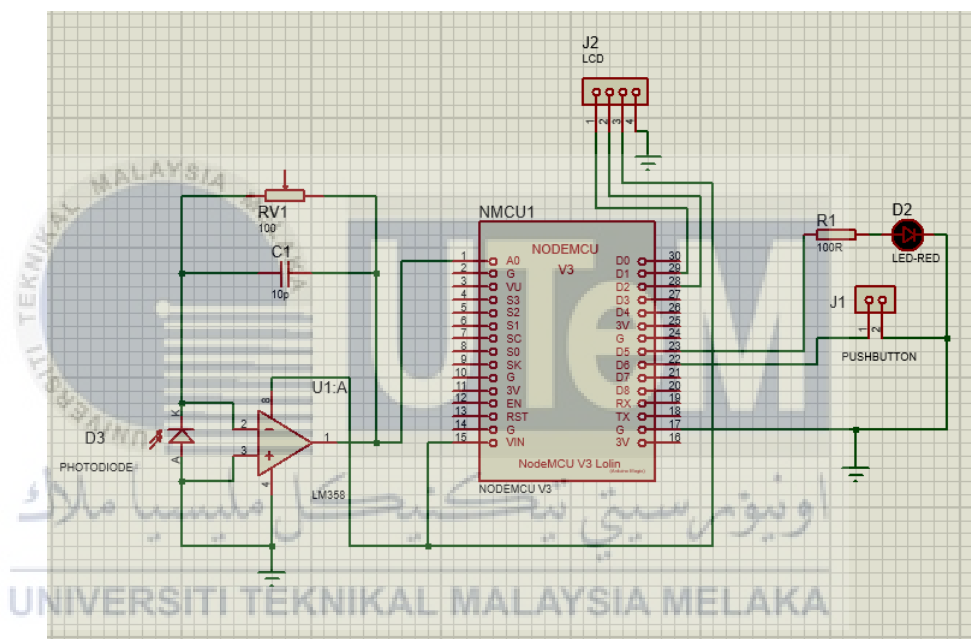


**Figure 3.5: Standard schematic diagram of the optical sensor based SPR**

For the PCB layout, all components must be positioned within the yellow border, which is also referred to as the board edge. The precise location of each component must be identified thoroughly in order to optimize circuit design development, which is quantified by the number of jumpers. The lesser the number of the jumper used, the better and there was none used in this instance. The circuit layout for the PCB is shown in the Figure 3.6 below with their respective label.

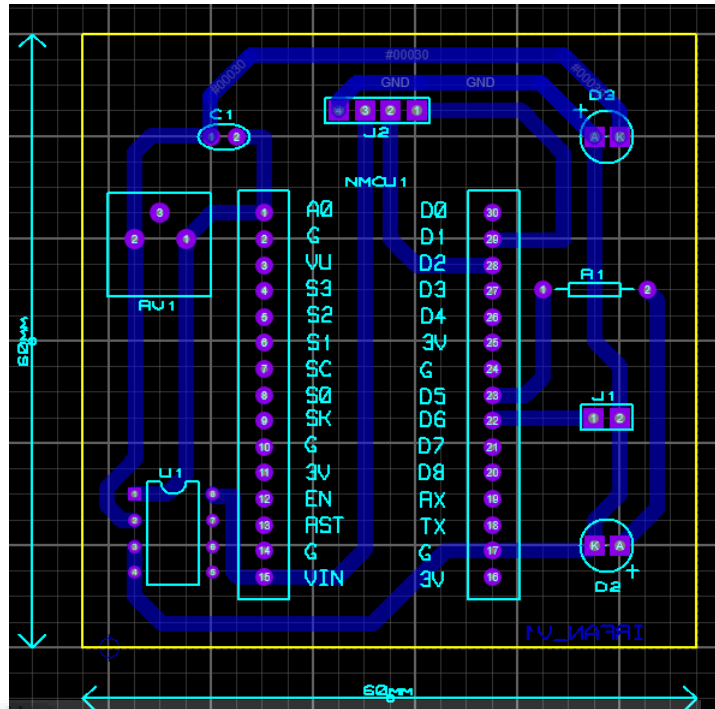


**Figure 3.6: Circuit layout that is printed on the UV Board**

After the designing process has been finalized, the circuit is printed on the UV Board and all required component's pins were soldered onto the board as displayed in Figure 3.7.



**Figure 3.7: Printed circuit onto the UV board**

After that, the other components required to complete the circuit including LED, LT1884(Op-Amp), i2C LCD Display, variable resistor, 1 k $\Omega$  resistor, push-button and the Nodemcu were integrated together as shown in Figure 3.8. Dupont Jumper Wires were used to connect the components that was not directly mounted onto the UV Board.

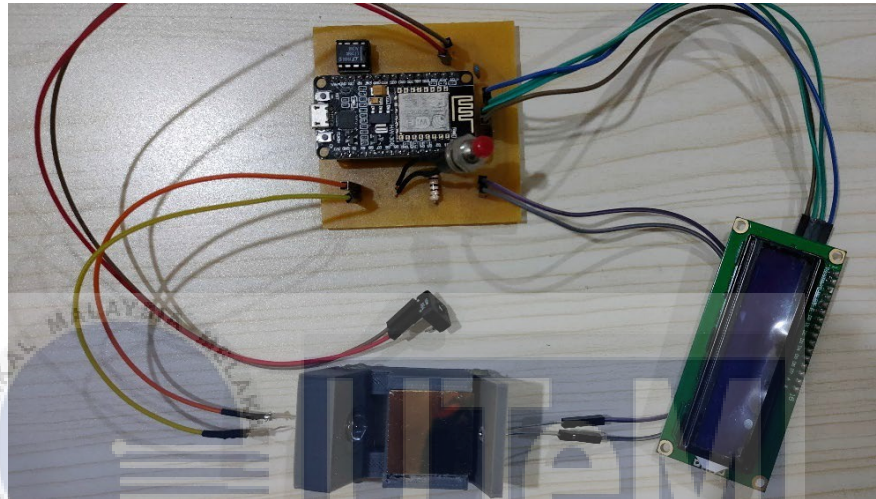


**Figure 3.8: Optical sensor based SPR circuit configuration**

اونيورسيتي تيكنيكل مليسيا ملاك

UNIVERSITI TEKNIKAL MALAYSIA MELAKA

### 3.2 Fabrication for SPR chip

The electron beam evaporation technique is utilised to create SPR chips, and the size of the SPR chip illustrated in Figure 3.9 is a result of that process. Glass substrate was placed on top of the machine with the surface facing down. Flux is deposited on the glass when the target substance has evaporated. This project used a 2.5 cm x 2.5 cm grid and a 30 mm deposition layer. Fig. 3.10 depicts the University of Malaya's electron beam evaporation (EBE) machine.

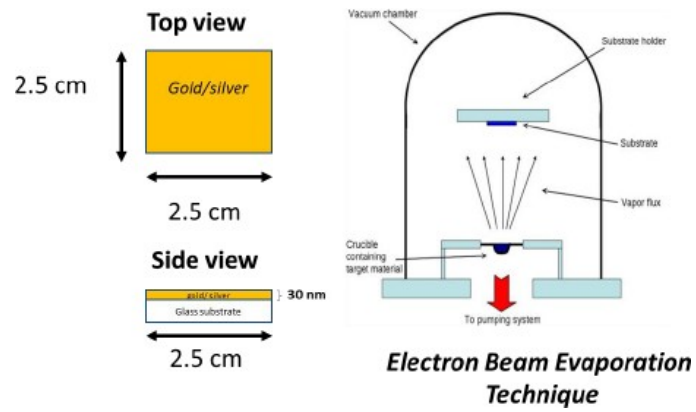


**Figure 3.9: SPR chip's size and coating technique**



**Figure 3.10: Machine used for coating SPR chips**

### 3.3 Optical sensor based SPR circuit IoT integration process

In this project, the raw data of the transmitted light received by the photodetector is expected to be send into the e-mail. For that purpose, an app called Blynk (Figure 3.12) is used to connect the designed circuit with the email via Wi-Fi. Initially, a configuration must be set up before the microcontroller (Nodemcu) may be used to carry out the function in concern, and this is done by developing the coding used in the application. The coding can be observed in Figure 3.11 below.

```
//-----GLOBAL DECLARE-----
LiquidCrystal_I2C lcd(0x27, 16, 2);
int Red_LED= 14;
int PushButton= 12;
int buttonState = 0;
int customDelay = 200;
int analogPin = A0;//Photodiode Pin
int i;
//-----
//-----WIFI-SETUP-----
char auth[] = "FjPA2ovpMD1eJ7kb9n17dO2zu6OKJG6a"; //get from email
//Wi-Fi Credentials
char ssid[] = "xx";
char pass[] = "xxx";
//-----
void setup(){
//-----IO PIN DECLARATION-----
pinMode(Red_LED, OUTPUT);
pinMode(PushButton, INPUT);
pinMode(analogPin, INPUT);
//-----
//-----LCD INITIALIZATION-----
lcd.init();
lcd.setBacklight((uint8_t)1); // Enable or Turn On the backlight
lcd.setCursor(1,0);
lcd.print("Photodetector");
// Second row
lcd.setCursor(4,1);
lcd.print("Circuit");
delay(3000);
lcd.clear();
```

Figure 3.11: Some of the command lines developed in Arduino IDE software

The code that has been successfully developed was then flashed into the microcontroller (Nodemcu) to allow the Blynk app to connect with it later. Meanwhile, in the Blynk app, a function called SuperChart is used which it will displayed the received data in the form of graph as depicted in Figure 3.12 below.

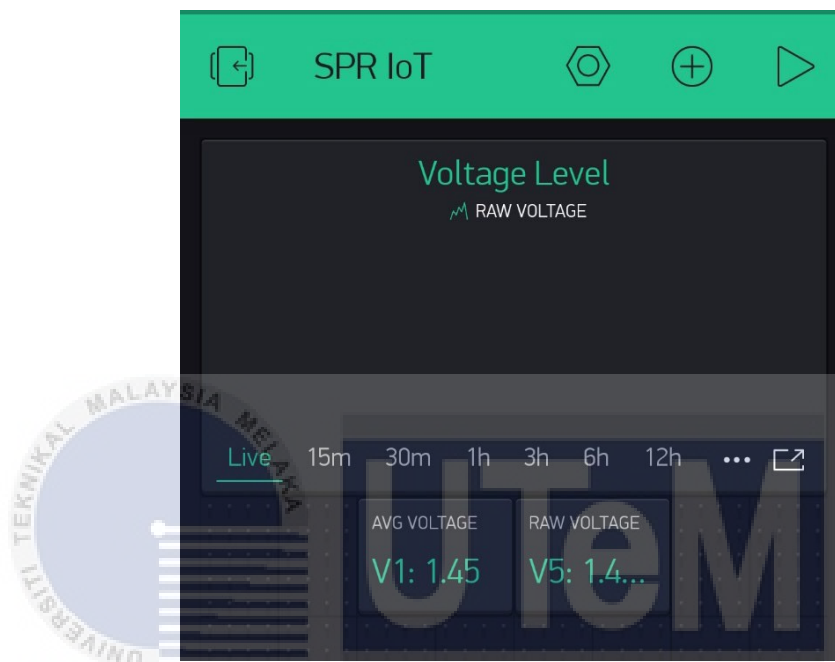
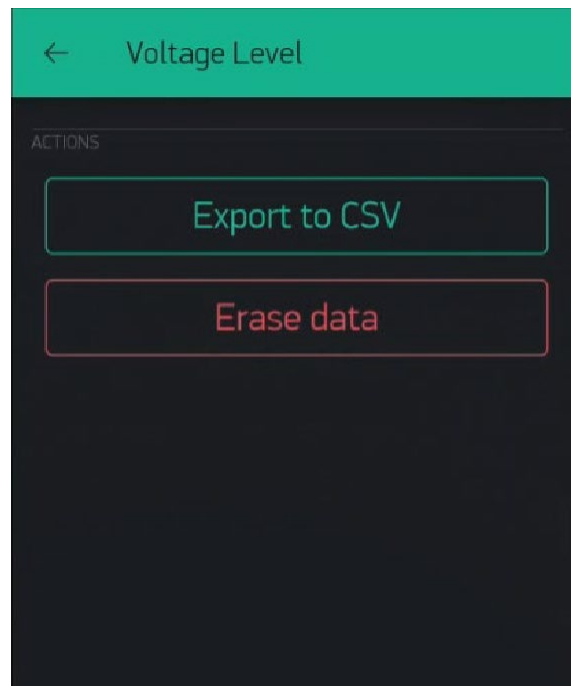


Figure 3.12: Blynk App with the SuperChart function

The raw data of the output voltage will be continuously received by the apps as long as the circuit is operated but as for the analysis, the limit of data received is set to be at 100 readings. So, whenever the number of data readings has met the requirements, the data of the raw output voltage has to be manually exported into the specified e-mail in the form of excel files by clicking the export button as depicted in Figure 3.13. This process has to be repeated for several times for each salinity concentration from 2% up to 12% and di-ionized water.



**Figure 3.13: Export function in the Blynk app**

Then, using the processes outlined in Figure 3.14, a series of experiments on the constructed optical sensor for characterization and analysis were carried out to evaluate the optical sensor's performance based on the SPR idea.

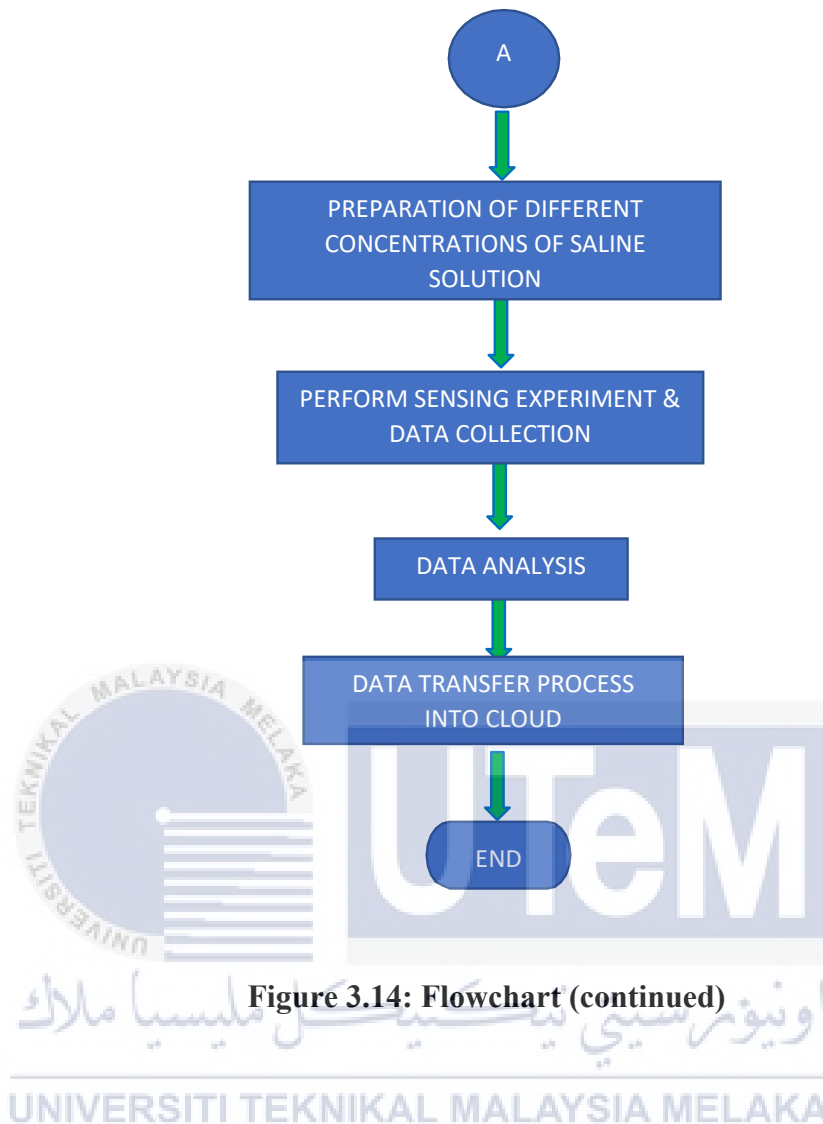


**Figure 3.14: Flowchart (continued)**

### 3.4 Solution Preparation and Sensing Process

Sodium Chloride, often known as saline solution, is the intended medium for this experiment, hence it must be made appropriately and using the suitable procedure. There were six salinity solutions prepared, ranging from 2% to 12%, and a di-ionized water. Both the saline and di-ionized water were taken from the lab as shown in Figure 3.15. At the same time, in Figure 3.16, there were 7 different bottles for storing the different salinity concentrations that were prepared with an appropriate label on each of them.

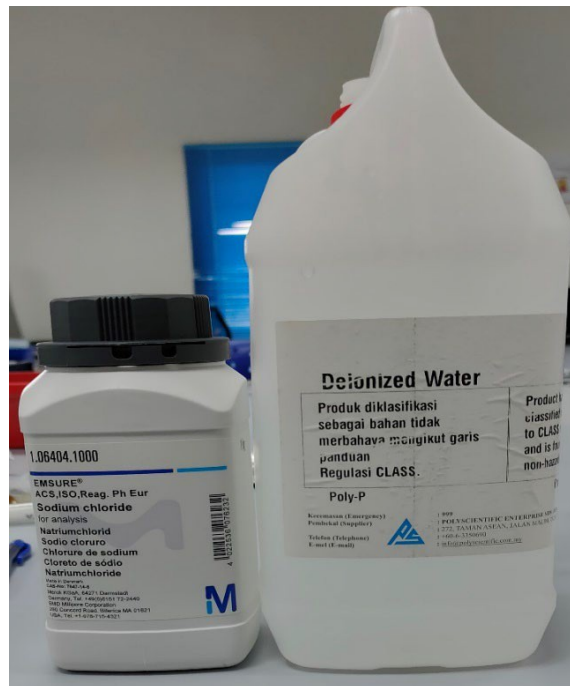


Figure 3.15: Sodium Chloride and De-ionized Water



Figure 3.16: The bottles for storing different salinity concentrations

Each of the salinity concentration was determined by measuring them on scale that have a high sensitivity on mass (Figure 3.17) before mixing them with the de-ionized water by using the Heating Magnetic Stirrer as shown in Figure 3.18.



**Figure 3.17: Scale for measuring the Sodium Chloride**



**Figure 3.18: Heating Magnetic Stirrer**

After all the solutions have been mixed together with the de-ionized water for every salinity concentration mentioned before, the refractive index for each of them were measured by using the Digital Refractometer (Figure 3.19).



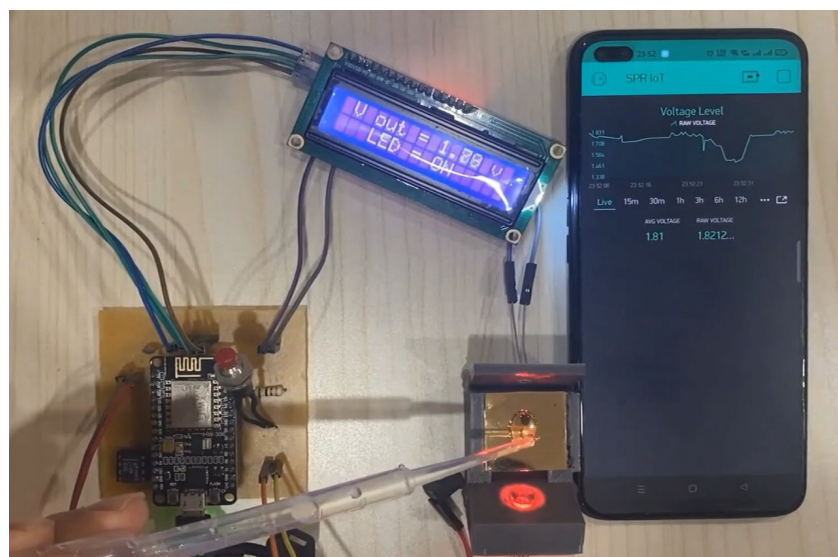
Figure 3.19: Digital Refractometer

As for the results of this process, the refractive index unit of pure de-ionized water is 1.333 RIU, whereas the other salinity solutions with varying concentrations have refractive index units shown in Table 3.1.

**Table 3.1: Salinity solution with different concentrations and its RIU**

Salinity Concentration (%)	Refractive Index Unit (RIU)
2	1.335
4	1.340
6	1.344
8	1.348
10	1.350
12	1.354

Then, in the sensing process, each of the solution was dropped onto the SPR chip as portrayed in Figure 3.20. An approximate of 5 drops were used for each salinity solution and then it was left on the SPR chips for a while in order to allow the photodetector to make the 100 readings of the transmitted light. The process was then repeated until all the solution with 2% up to 12% concentrations have been analyzed.

**Figure 3.20: Demonstration of the solution dropping onto the SPR chip**

## CHAPTER 4

### RESULTS AND DISCUSSION

This chapter explains in detail the analysis process of the proposed optical sensor in order to achieve the three objectives of this research work. First and foremost, the LED light source and photodetector circuit was analysed in order to ensure that the circuit is working as planned. Then, the designed circuit was integrated with the IoT platform by using Blynk app as the medium. Once the IoT integration working as expected, the sensing performance of the optical sensor based SPR was performed with the IoT platform to sense the different of the saline solution concentrations and the sensing performance was analyzed.

#### 4.1 Analysis of The Designed Circuit and Internet of Thing (IoT) Integration.

As the LED light source was launched directly to the photodetector, the light was detected and amplified before being displayed on the LCD as shown in Figure 4.1. The maximum output voltage received by the photodetector is 5V due to the LT1884 (op-amp) specifications. Prior to sensing saline concentration, the output voltage was set at 1.604 V in air since the voltage is predicted to rise as saline concentration increases.



**Figure 4.1: Circuit's Configuration**

After the IoT successfully integrated with the LED and photodetector circuit, its performance was analysed in order to monitor the output voltage displayed on the apps interface (Blynk) as shown in Figure 4.2, the displayed output voltage has been

averaged by the equation set on the command lines from Arduino IDE software in the microcontroller (Nodemcu) for 100 readings. The graph as shown in Figure 4.2 indicates the variation of the raw output voltage detected by the photodetector. It means that the IoT integration has been successfully integrated.

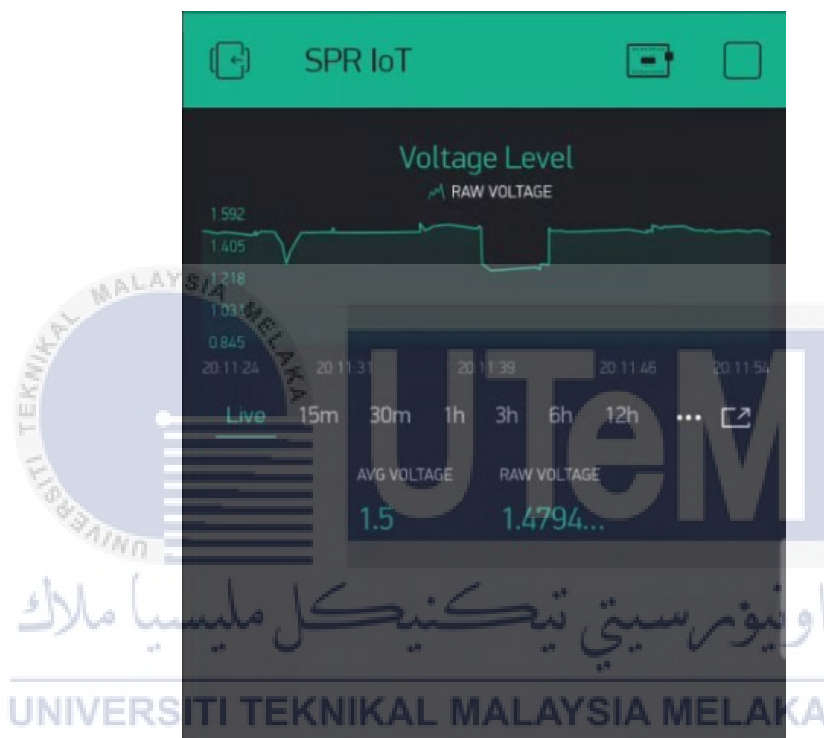


**Figure 4.2: The interface of the Blynk app with the running data received from the optical sensor circuit**

As explained in chapter 3, Figure 4.3 shows the exported data of the average output voltage formatted in excel file type. The total of the data recorded in the excel is exactly 100 readings of the average output voltage. The data was used for the sensing performance analysis as discussed in next sub-topic.

	A	B	C	D	E	F
1	1.38817	1.6E+12	0			
2	1.3863	1.6E+12	0			
3	1.41317	1.6E+12	0			
4	1.48956	1.6E+12	0			
5	1.51806	1.6E+12	0			
6	1.50502	1.6E+12	0			
7	1.48827	1.6E+12	0			
8	1.49764	1.6E+12	0			
9	1.53727	1.6E+12	0			
10	1.58478	1.6E+12	0			
11	1.65522	1.6E+12	0			
12	1.78039	1.6E+12	0			
13	1.94242	1.6E+12	0			
14	2.1127	1.6E+12	0			
15	2.25355	1.6E+12	0			
16	2.33126	1.6E+12	0			
17	2.36737	1.6E+12	0			
18	2.45073	1.6E+12	0			
19	2.51854	1.6E+12	0			
20	2.58618	1.6E+12	0			
21	2.65623	1.6E+12	0			
22	2.73319	1.6E+12	0			
23	2.80006	1.6E+12	0			
24	2.87657	1.6E+12	0			
25	2.94377	1.6E+12	0			
26	2.95928	1.6E+12	0			
27	2.99447	1.6E+12	0			
28	2.97943	1.6E+12	0			
29	2.97543	1.6E+12	0			
30	2.95927	1.6E+12	0			

Figure 4.3: Array of received output voltage

#### 4.2 Analysis of The Optical Sensor Based SPR With IoT Platform for Solution Concentrations Detection

Based on seven tests that have been carried out throughout the project's development, the results collected were analyzed to validate the sensing performance such as sensitivity, linearity, standard deviation and resolution.

For the experiment wise, 6 different salinity concentrations, air and de-ionized water were prepared as explained in chapter 3. Initially, the results in term of output voltage are expected to be higher whenever the salinity concentrations are higher. This

conclusion is based on the research which shows that adding salt or saline into the water increases its conductivity as the salt act as the electrolyte. The more conductivity there is, the better the flow of electricity will be. With more electrolyte in the solution, the voltage output is expected to be higher.

For each salinity concentrations, an approximate of 100 readings of the output voltage were made. Then, the raw data of the output voltage were compiled together for further analysis by using Microsoft Excel software which then the average output voltage and standard deviation were generated. After that, a graph of normalised average output voltage (V) against salinity solution concentration (g) is created as shown in Figure 4.4

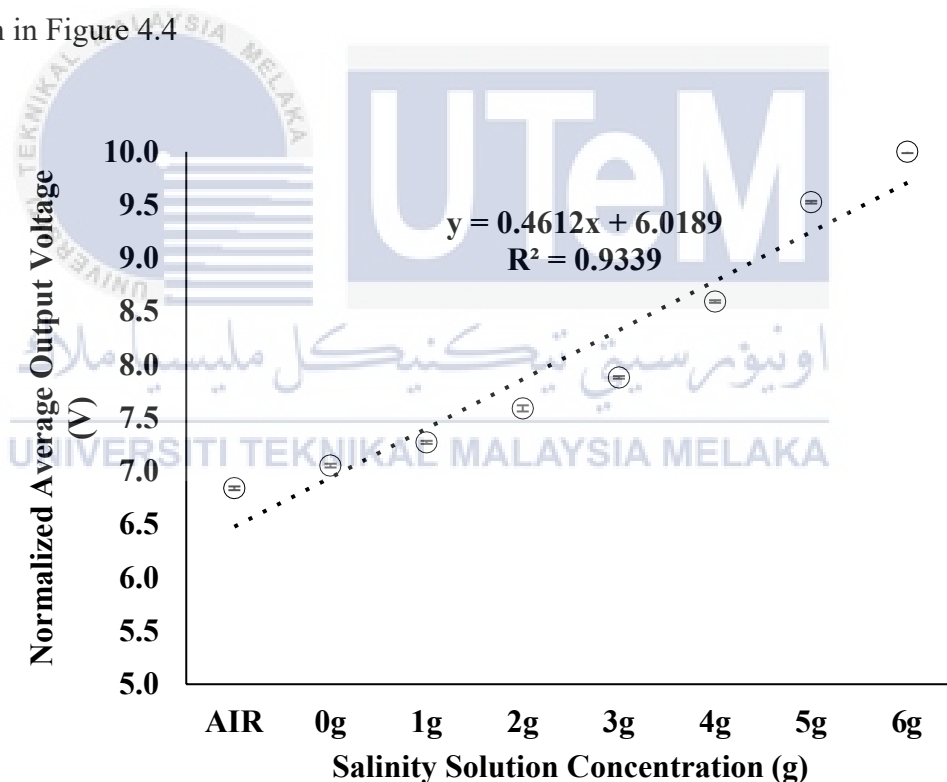


**Figure 4.4: Normalized average output voltage against salinity solution concentration (g)**

From the figure above, the average output voltages received from the photodetector which is proportional to the transmitted light increases linearly as the concentrations of the salinity solution increases. Meanwhile, the sensitivity is obtained at 0.4612 V/g and attained a good linearity on the slope which at 93.39%. Figure 4.5 shows the normalized average output voltage (V) against salinity solution concentration (%). It indicates the same sensitivity and linearity as the previous graph.

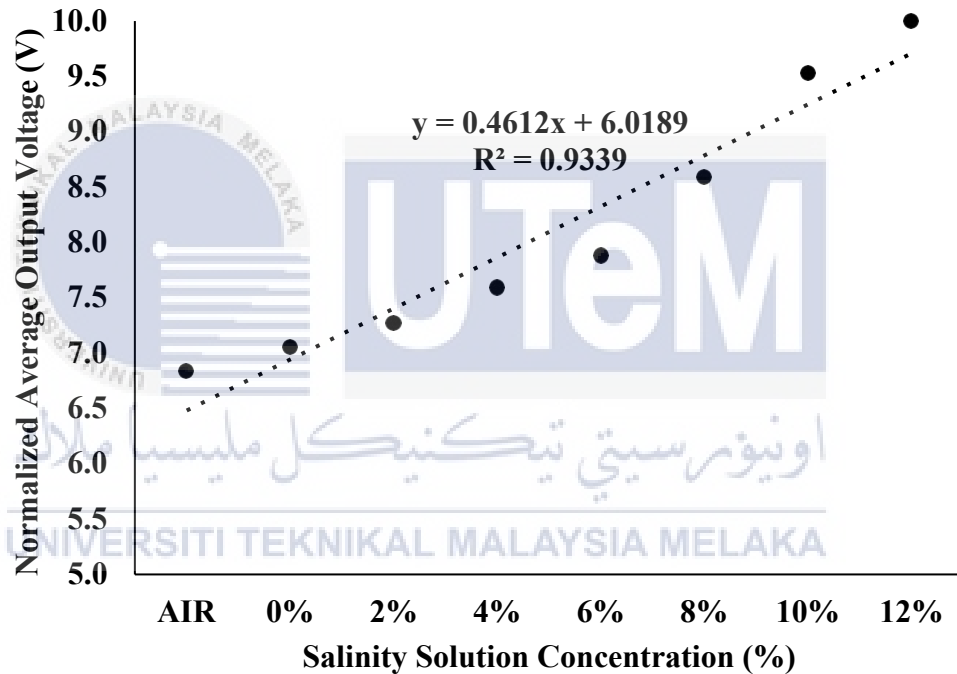


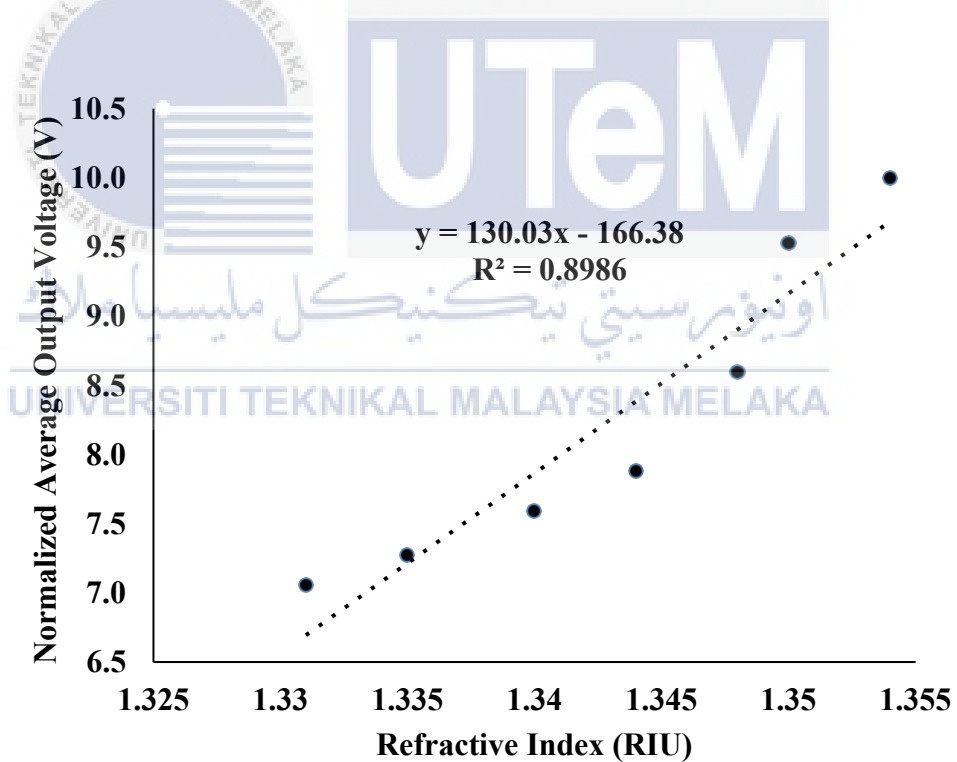
**Figure 4.5: Normalized average output voltage against salinity solution concentration (%)**

The sensor performances were then tabulated into table 4.1. To be precise, the table includes sensitivity (V/%), linearity (%), standard deviation (V), and the resolution (RIU).

**Table 4.1: The performance of the optical sensor on the salinity solution**

SENSOR PERFORMANCE	
SENSITIVITY (V/%)	0.4612
LINEARITY (%)	93.39
STANDARD DEVIATION (V)	1.169
RESOLUTION (RIU)	0.063036

Then, Figure 4.6 shows the normalized output voltage against the refractive index unit (RIU). As the concentration of the salinity solution increase from 0% to 12%, the refractive index also increases from 1.333ri to 1.354 RIU.

**Figure 4.6: Normalised average output voltage (V) against refractive index unit (RIU)**

The sensor performance is summarized in Table 4.2 Overall, the sensor is observed to be sufficiently stable with a standard deviation of 1.169V while being recorded for 100 readings. These results suggest that the proposed sensor is practical and beneficial for salinity detection, especially in the industry, due to the sensor's capacity to provide real-time salinity detection and control of diverse combinations.

**Table 4.2: Sensor performance of the optical sensor with the refractive index**

SENSOR PERFORMANCE	
SENSITIVITY (V/RIU)	131.9
LINEARITY (%)	90.32
STANDARD DEVIATION (V)	1.169
RESOLUTION (RIU)	0.0002204

### 4.3 Sensing Mechanism

The sensing mechanism of this optical sensor is illustrated in Figure 4.7. The LED's light signal will arrive sporadically. Unpolarised light is the term used to describe this type of light. The light was then polarised by inserting a polarizer (thin plastic film) between the SPR chip and the LED. Additionally, the polarizer aids in obtaining the most amount of light signal possible. The light signal then refracts and reflects off the glass substrate until it reaches the end. The reflected light is the light that was not absorbed as a result of the reaction between the varying concentrations of saline solution and the electron in gold caused by the SPR phenomenon. The photodetector detected and turned the reflected light into an electrical signal. Finally, the electrical signal is shown on the LCD screen in form of voltage.

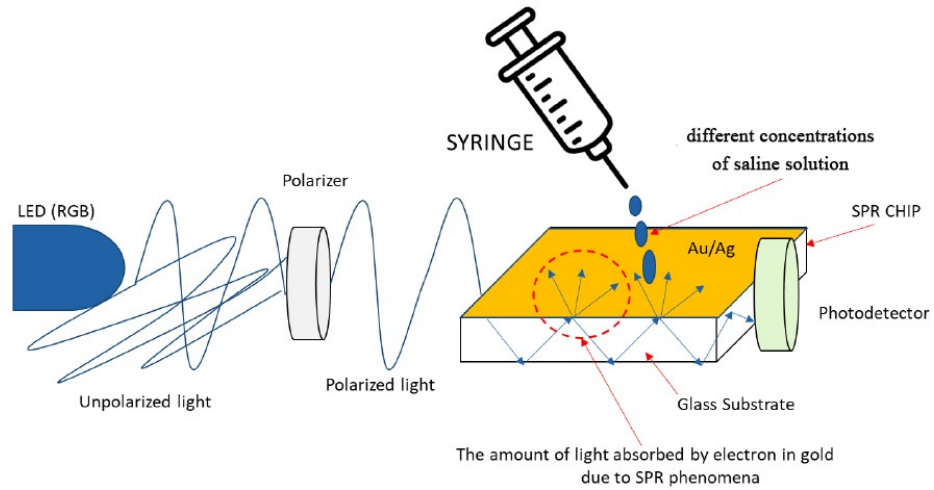
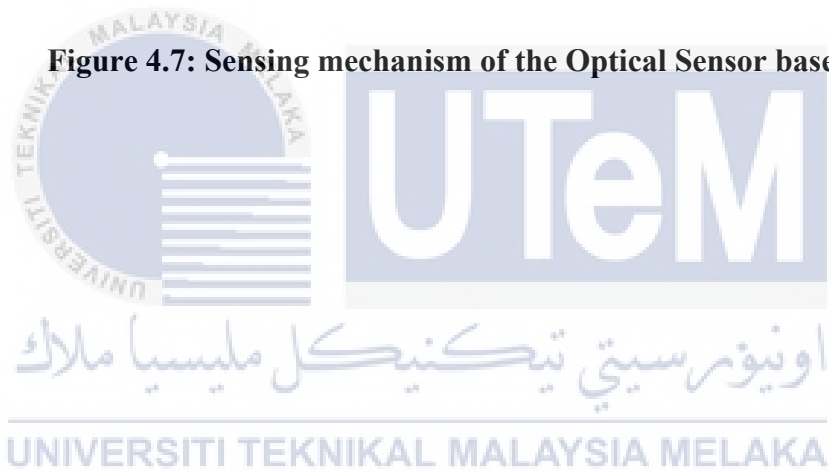


**Figure 4.7: Sensing mechanism of the Optical Sensor based SPR**



## CHAPTER 5

### CONCLUSION AND FUTURE WORKS



To summarize, this project met all three of its goals, and it shows how a low-cost and simple optical sensor based on SPR may be expanded to measure saline solution concentration. Nodemcu microcontroller's data processing platform was used to create a low-cost sensor device employing commercial LED as the light source and a low-cost photodiode. The higher the salinity solution concentration, the higher the voltage measured towards the SPR effect for gold, according to the results obtained.

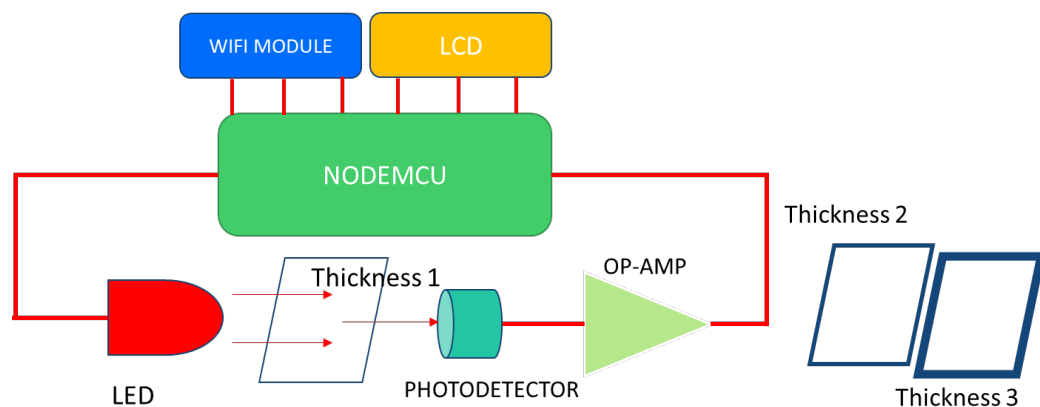
Based on the research paper wrote by H.A Rahman, Table 5.1 shows the comparison of sensor performances between her sensor and this proposed optical sensor based SPR for salinity concentration detection.

**Table 5.1: difference between H.A. Rahman sensor with this project optical sensor based SPR**

Parameter \ Optical Sensor	Rahman, H. A. (2011). [12]	Proposed optical sensor based SPR
Sensitivity (v/%)	$0.0024 \times 10^{-3}$	0.4612
Sensor Setup	<ul style="list-style-type: none"> <li>• complicated</li> <li>• use laser as light source</li> <li>• expensive</li> </ul>	<ul style="list-style-type: none"> <li>• simple</li> <li>• use LED</li> <li>• low cost</li> </ul>

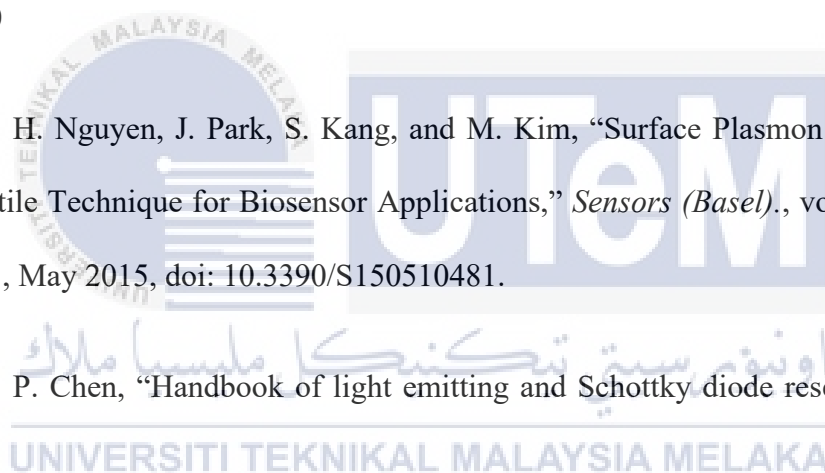
### 5.1 Future Works

For future work, this project's circuit can be used for other application that related to light characteristics such as reflection, refraction, absorption. It is not limited to measure solution concentration but it is also able to measure other physical parameters such as transparent material thickness and space area of a transparent object. Theoretically, different thickness of the transparent object will have a different light absorption rate.



**Figure 5.1: Block diagram of the optical sensor circuit for future work**

## REFERENCES

- [1] R. B. Schasfoort, "Chapter 3. Surface Plasmon Resonance Instruments," Handbook of Surface Plasmon Resonance, pp. 60–105. doi: 10.1039/9781788010283-00060
- [2] H. H. Nguyen, J. Park, S. Kang, and M. Kim, "Surface Plasmon Resonance: A Versatile Technique for Biosensor Applications," *Sensors (Basel)*, vol. 15, no. 5, p. 10481, May 2015, doi: 10.3390/S150510481.
- [3] N. P. Chen, "Handbook of light emitting and Schottky diode research," p. 621, 2009. 
- [4] B. H. Choi, H. H. Lee, S. Jin, S. Chun, and S. H. Kim, "Characterization of the optical properties of silver nanoparticle films," *Nanotechnology*, vol. 18, no. 7, 2007, doi: 10.1088/0957-4484/18/7/075706.
- [5] P. Englebienne, A. Van Hoonacker, and M. Verhas, "Surface plasmon resonance: Principles, methods and applications in biomedical sciences," *Spectroscopy*, vol. 17, no. 2–3, pp. 255–273, 2003, doi: 10.1155/2003/372913.

- [6] A. L. González and C. Noguez, "Optical properties of silver nanoparticles," *Phys. Status Solidi Curr. Top. Solid State Phys.*, vol. 4, no. 11, pp. 4118–4126, 2007, doi: 10.1002/pssc.200675903.
- [7] A. K. Khan, R. Rashid, G. Murtaza, and A. Zahra, "Gold nanoparticles: Synthesis and applications in drug delivery," *Trop. J. Pharm. Res.*, vol. 13, no. 7, pp. 1169–1177, 2014, doi: 10.4314/tjpr.v13i7.23.
- [8] H. H. Nguyen, J. Park, S. Kang, and M. Kim, "Surface plasmon resonance: A versatile technique for biosensor applications," *Sensors (Switzerland)*, vol. 15, no. 5, pp. 10481–10510, 2015, doi: 10.3390/s150510481.
- [9] Xia, F., Yang, L. T., Wang, L., & Vinel, A. (2012). Internet of Things. *International Journal of Communication Systems*, 25(9), 1101–1102. <https://doi.org/10.1002/dac.2417>
- [10] Karen, R., Scott, E., & Lyman, C. (2015). THE INTERNET OF THINGS: AN OVERVIEW. *Internet Of Things*. Published.
- [11] Dachyar, M., Zagloel, T. Y. M., & Saragih, L. R. (2019). Knowledge growth and development: internet of things (IoT) research, 2006–2018. *Heliyon*, 5(8), e02264. <https://doi.org/10.1016/j.heliyon.2019.e02264>
- [12] Rahman, H., Harun, S., Yasin, M., Phang, S., Damanhuri, S., Arof, H., & Ahmad, H. (2011). Tapered plastic multimode fiber sensor for salinity detection. *Sensors and Actuators A: Physical*, 171(2), 219–222. <https://doi.org/10.1016/j.sna.2011.09.024>

[13] DAVID, M., & FLORESCU, M. (2016). BIOMOLECULAR INTERACTION EVALUATION USING SURFACE PLASMON RESONANCE. SPR BIOSENSORS. *Biophysics for Biomedical and Environmental Sciences*, 211.

[14] B. A. Prabowo, A. Purwidyantri, and K. C. Liu, "Surface Plasmon Resonance Optical Sensor: A Review on Light Source Technology," *Biosens. 2018, Vol. 8, Page 80*, vol. 8, no. 3, p. 80, Aug. 2018, doi: 10.3390/BIOS8030080.

[15] P. O. Patil *et al.*, "Graphene-based nanocomposites for sensitivity enhancement of surface plasmon resonance sensor for biological and chemical sensing: A review," *Biosens. Bioelectron.*, vol. 139, p. 111324, Aug. 2019, doi: 10.1016/J.BIOS.2019.111324.

[16] Y. Yuan *et al.*, "Fiber Grating-Assisted Surface Plasmon Resonance for Biochemical and Electrochemical Sensing," *J. Light. Technol. Vol. 35, Issue 16, pp. 3323-3333*, vol. 35, no. 16, pp. 3323–3333, Aug. 2017, doi: 10.1021/ACS.ANALCHEM.6B01314.

[17] W. Diao *et al.*, "Highly sensitive surface plasmon resonance biosensor for the detection of HIV-related DNA based on dynamic and structural DNA nanodevices," *Biosens. Bioelectron.*, vol. 100, pp. 228–234, Feb. 2018, doi: 10.1016/J.BIOS.2017.08.042.

[18] A. Paliwal, M. Tomar, and V. Gupta, "Table top surface plasmon resonance measurement system for efficient urea biosensing using ZnO thin film matrix,"

<https://doi.org/10.1117/1.JBO.21.8.087006>, vol. 21, no. 8, p. 087006, Aug. 2016, doi: 10.1117/1.JBO.21.8.087006.

[19] H. H. Nguyen, J. Park, S. Kang, and M. Kim, “Surface Plasmon Resonance: A Versatile Technique for Biosensor Applications,” *Sensors (Basel)*, vol. 15, no. 5, p. 10481, May 2015, doi: 10.3390/S150510481.

[20] T. Jiang, M. Minunni, P. Wilson, J. Zhang, A. P. F. Turner, and M. Mascini, “Detection of TP53 mutation using a portable surface plasmon resonance DNA-based biosensor,” *Biosens. Bioelectron.*, vol. 20, no. 10, pp. 1939–1945, Apr. 2005, doi: 10.1016/J.BIOS.2004.08.040.

[21] M. R. Krames and R. D. Dupuis, “History, Development, and Applications of High-Brightness Visible Light-Emitting Diodes,” *J. Light. Technol. Vol. 26, Issue 9*, pp. 1154–1171, vol. 26, no. 9, pp. 1154–1171, May 2008, Accessed: Jan. 11, 2022. [Online]. Available: <https://www.osapublishing.org/abstract.cfm?uri=jlt-26-9-1154>.

[22] M. Moznuzzaman, M. Rafiqul Islam, M. Biplob Hossain, and I. Mustafa Mehedi, “Modeling of highly improved SPR sensor for formalin detection,” *Results Phys.*, vol. 16, p. 102874, Mar. 2020, doi: 10.1016/J.RINP.2019.102874.

[23] C. Huang *et al.*, “Localized surface plasmon resonance biosensor integrated with microfluidic chip,” *Biomed. Microdevices 2009 114*, vol. 11, no. 4, pp. 893–901, Apr. 2009, doi: 10.1007/S10544-009-9306-8.

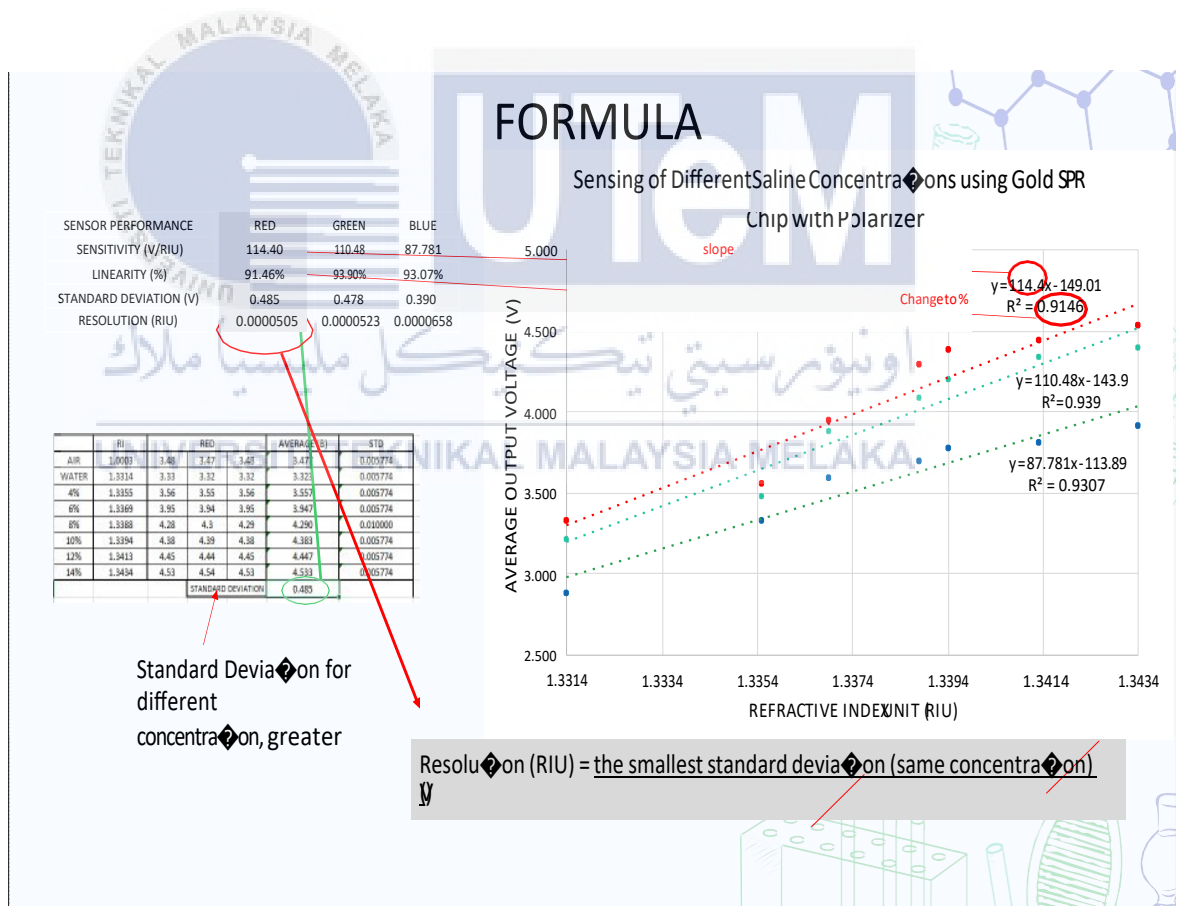
[24] “IEEE Internet of Things Journal - IEEE Internet of Things Journal.” <https://iee-iotj.org/> (accessed Jan. 11, 2022).

- [25] S. Aleksic, “A survey on optical technologies for IoT, smart industry, and smart infrastructures,” *J. Sens. Actuator Networks*, vol. 8, no. 3, 2019, doi: 10.3390/JSAN8030047.
- [26] J. H. Valente, R. J. Forti, L. F. Freundlich, S. O. Zandieh, and E. F. Crain, “Wound irrigation in children: Saline solution or tap water?,” *Ann. Emerg. Med.*, vol. 41, no. 5, pp. 609–616, May 2003, doi: 10.1067/MEM.2003.137.
- [27] “Side Effects of Normal Saline (Sodium Chloride Injection), Warnings, Uses.” <https://www.rxlist.com/normal-saline-side-effects-drug-center.htm> (accessed Jan. 7, 202



# APPENDIX A

## FORMULA USED IN ANALYSIS



## APPENDIX B

### CODING FOR NODEMCU

```
//.....LIBRARY.....
```

```
#include <LiquidCrystal_I2C.h>
```

```
#include <ESP8266WiFi.h>
```

```
#include <BlynkSimpleEsp8266.h>
```

```
#include <SoftwareSerial.h>
```

```
#define BLYNK_PRINT Serial
```

```
//.....
```

```
//.....GLOBAL DECLARE.....
```

```
LiquidCrystal_I2C lcd(0x27, 16, 2);
```

```
int Red_LED= 14;
```

```

int PushButton = 12;

int buttonState = 0;

int customDelay = 200;

int analogPin = A0;//Photodiode Pin

int i;

//.....

//.....WIFI-SETUP.....

char auth[] = "uniquecodegivenbyblynk";//get from email

//Wi-Fi Credentials
char ssid[] = "xxxxx";

char pass[] = "yyyyy";

//.....

void setup(){

//.....IO PIN DECLARATION.....

```

```
pinMode(Red_LED, OUTPUT);

pinMode(PushButton, INPUT);

pinMode(analogPin, INPUT);

//.....

//.....LCD INITIALIZATION.....

lcd.init();

lcd.setBacklight((uint8_t)1); // Enable or Turn On the backlight

lcd.setCursor(1,0);

lcd.print("Photodetector");

// Second row

lcd.setCursor(4,1);

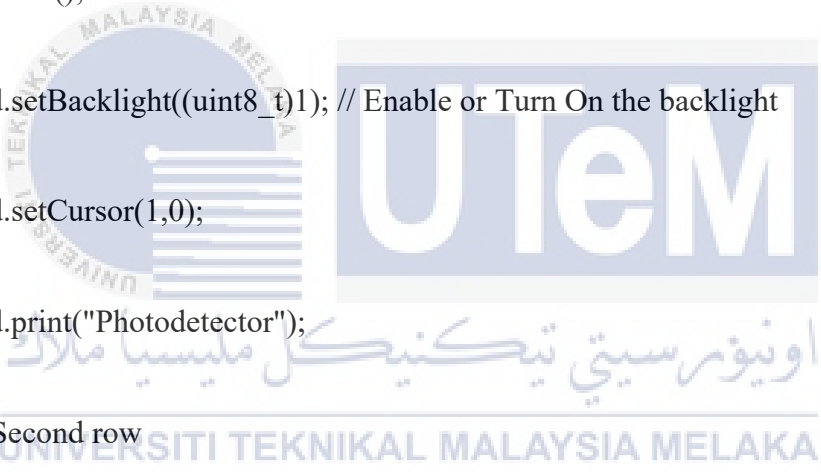
lcd.print("Circuit");

delay(3000);

lcd.clear();

lcd.setCursor(1,1);

//.....
```



```
Serial.begin(9600);
```

```
Serial.println("Led is turned off");
```

```
Blynk.begin(auth, ssid, pass);
```

```
}
```

```
void loop(){
```

```
Blynk.run();
```

```
//delay(1000);
```

```
//Blynk.email("xyxyxy@gmail.com", "ESP8266 Alert!", "Voltage Detected ");
```

```
//-----push button reading process-----
```

```
//for (int pin = 2; pin <=13; pin++){
```

```
  //pinMode(pin, OUTPUT);
```

```
// }
```



```
pinMode(PushButton, INPUT_PULLUP);
```

```
buttonState = digitalRead(PushButton);
```

```
if(buttonState == LOW){
```

```
    i++;
```

```
    delay(200);
```

```
    if(i == 1){
```

```
        Serial.println("LED turned ON");
```

```
        digitalWrite(14, HIGH);
```

```
        lcd.setCursor(3,1);
```

```
        lcd.print("LED = ON ");
```

```
        delay(500);
```

```
    }
```

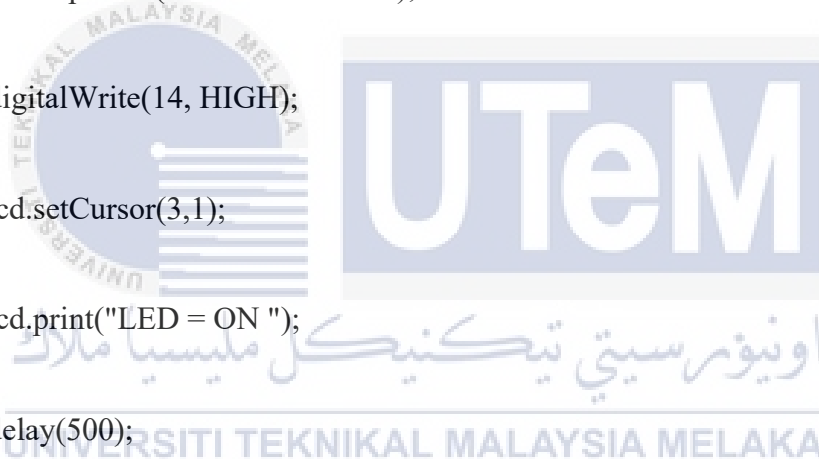
```
    else if (i == 2){
```

```
        Serial.println("LED turned OFF");
```

```
        digitalWrite(14, LOW);
```

```
        lcd.setCursor(3,1);
```

```
        lcd.print("LED = OFF");
```



```

i=0;

delay(500);

}

}

//.....

//-----average calculation process-----

int maxvoltReads = 20; //max number of samples
int voltReads = 0; // initial condition of the sample
for (int k = 0; k < maxvoltReads; k++){
    voltReads += analogRead(analogPin);

    delay(1);

}

float newvolt = voltReads * (5.0 / 1024.0);

float avg = newvolt / maxvoltReads;

//float avgvolt = avg * (5.0 / 1024.0); // convert the raw data value(0 - 1023) to
voltage (0.0V - 5.0V)

```

```
Serial.println(avg);

Serial.print(analogRead(analogPin)* (5.0 / 1024.0));

Serial.print('\t');

//Serial.print(random(16000), HEX);

//-Serial.print('\n');

delay(1);

//.....

lcd.setCursor(1,0);
lcd.print("V out = ");
lcd.setCursor(9,0);
lcd.print(avg);

lcd.setCursor(14,0);

lcd.print("v");

delay(250);

Blynk.virtualWrite(V5, analogRead(analogPin)* (5.0 / 1024.0));

Blynk.virtualWrite(V1, avg); }
```